Combining physical and geochemical methods to investigate lower halocline water formation and modification along the Siberian continental slope

Matthew B. Alkire[1], Igor Polyakov[2], Robert Rember[2], Andrey Pnyushkov[2], Vladimir Ivanov[3, 2], Igor Ashik[3]

[1]Applied Physics Laboratory, University of Washington, Seattle, WA USA
[2]International Arctic Research Center, University of Alaska Fairbanks, Fairbanks, AK USA
[3]Arctic and Antarctic Research Institute, St. Petersburg, RUS

Correspondence to: Matthew B. Alkire (malkire@apl.washington.edu)

Responses to Reviewer Comments

We thank the two reviewers for their helpful suggestions and comments regarding this manuscript. As a result of these comments, we have undertaken significant revisions of the paper, both in the revision and addition of figures and a significant expansion of the text to further clarify major discussion points. We have also moved some tables from the Supplementary Information to the main text, in support of this expanded discussion.

We have addressed each of the comments provided by the two reviewers. Our responses are located directly below each specific comment, in bold type. Page and line numbers mentioned in our responses refer to a revised version of the manuscript that we have prepared and are ready to submit for consideration.

Anonymous Referee #1

This manuscript examines the importance of river water and sea-ice melt/brine in lower halocline water (LHW) formation through mixing. The study is based on observations/sampling in the Eurasian basin of the Arctic Ocean and along the continental slope of the Kara, Laptev, and East Siberian Seas during summers of 2013 and 2015. The study, which uses δ18O along with CTD measurements, suggests that LHW is formed by convective mechanisms with two stages of convective mixing during the transit along the continental slope and thus offers an alternative hypothesis to the study published by Bauch et al. (2016). The Alkire study makes an important contribution to the understanding of the mechanism which may impact the vertical heat fluxes between the (seasonally) ice covered surface layer and the underlying "warm" Atlantic water (AW). The paper is concise, well structured, and well written.

Thank you.

The main issue that needs to be addressed is the result presented in the last sentence of the abstract. The authors postulate that: "These mixing regimes appear to have been

robust since at least 2000". This means that the mixing regimes are stable although the region experienced significant changes in sea ice cover and temperature/volume of AW during the last two decades (references in the manuscript). Does that also mean that the intensity of vertical mixing between LHW and AW has not changed since 2000?

No, this does not mean that the intensity of vertical mixing between LHW and AW has not changed since 2000. We apologize for the confusion and thank the reviewer for pointing out this obscurity. We argue that the apparent consistency of the mixing regimes, as defined by the salinity-d18O mixing lines, indicate that the processes responsible for the formation of halocline waters has remained more-or-less constant regardless of the large and important environmental changes observed over the Arctic Ocean during the past two decades. Although the spatial distribution and strength of stratification provided by the halocline may have been altered, the processes responsible for halocline water formation have apparently not changed.

We have added a new section (4.3) as well as an additional paragraph at the end of the paper (Page 11, Lines 24-32) that provides further context supporting our conclusion.

Considering the importance of these conclusions I'm not convinced that they are a result of the analysis presented in this paper. The authors state that the conclusion was drawn based on a comparison against other data sets (?) collected between 2000 and 2015 (page 8, line 14). This description seems too vague to me. It should be discussed in more detail.

The data sets collected between 2000 and 2015 are those presented in Figure 6 of the revised manuscript. They include data collected in 2013 and 2015 (presented in this study) as well as from the North Pole Environmental Observatory (2000-2015), ARK-XXII/2 (2007), and O-18 Atlas (1967-2008). The locations of observations collected during these programs are shown in Figure 2 of the revised manuscript.

We have added a section (4.3) to the revised manuscript that discusses the comparison in further detail.

Technical corrections:
The citation "Janout et al. (2015)" from the list of references is missing in the text/figures.

This citation has been deleted from the list of references.

The citation "Rudels et al. (1994)" from the list of references is missing in the text/figures.

This citation has been deleted from the list of references.

Is it Guay et al 2001 (text) or 2011 (references)?

The citation in the text is correct (2001) and has been corrected in the references.

The map shown in figure 1 is to small (at least for me). Maybe it would be better to show a map of the entire Arctic Ocean with the research area highlighted. Because this is the first map presented in the manuscript you should add longitude and latitude.

A larger map has been added as a new figure (Figure 2) in the revised manuscript.

Anonymous Referee #2

This manuscript addresses the Arctic Ocean halocline, its formation and evolution in the eastern Nansen and Amundsen basins. By the use of oxygen-18 data in combination with standard ctd measurements a front in the halocline characteristics is identified north of Severnaya Zemlya. West of the front sea ice melt water dominates in the halocline, while east of the front a stronger presence of meteoric water (runoff & precipitation) is observed. The stronger influence of meteoric water is due to vertical mixing with overlying, less saline water, but I am not sure if the authors also claim that the presence of meteoric water indicates major different sources of the halocline water.

We do not claim that the presence of meteoric water indicates major differences in the source(s) of halocline water. Instead, we utilize the available data to generally confirm the "convective mechanism" of halocline water formation that was previously postulated by Rudels et al. (1996). The front indicates an important geographic region where the "seasonal halocline" begins a transformation to the "permanent halocline".

We have significantly expanded the discussion in sections 4.1 and 4.2 and added text to the Abstract (Page 1, Lines 13-15) to further clarify this point.

Instead of discuss this issue here, I will first go through the manuscript from the top and then return to this question below.

Specific points: Page 1, lines 26-27: The halocline is not just the "kink" but also includes the water of different TS slope (stronger salinity change) up to the level of the seasonal deepening in winter, if lucky to be identified by a temperature minimum. It should perhaps also be stated that the lower halocline water was introduced by Jones and Anderson (1986) to distinguish it from the nutrient rich upper halocline with salinity around 33.1.

We have revised the text to better define the halocline as suggested by the reviewer and have included a citation for Jones and Anderson (1986). These additions can be found between Pages 1 (Line 26) and 2 (Line 9) of the revised manuscript.

Page 2, lines 6-8: In this scenario the upper layer is formed by melting sea ice and mixing the melt water into the upper part of the Atlantic water creating a fairly saline, cold upper layer. As the upper layer is advected eastward seasonal sea ice melt creates a summer halocline, which is removed by ice formation and brine release in winter, creating a winter mixed layer above the Atlantic water. As a general remark, I think that the use of an advected halocline versus a convective halocline complicates the picture. The winter mixed layer is advected and homogenized until it becomes covered by an outflow of less saline shelf water. If the shelf water is more saline and denser than the surface layer, it is injected into the water column below the upper layer. In both cases advection as well as convection are involved.

The reviewer makes an excellent point and we have added text to the manuscript pointing out this problem with the typical "advective" and "convective" labels of halocline water formation presented in the scientific literature (Page 2, Lines 16-28) and offer the terms of "shelf-derived" and "basin-derived" halocline waters instead.

Page 2, lines 11-13: As this description stands, it does not differ from the mechanism described in the paragraph above. As I interpret the schematics in Steele and Boyd (1998) the advective contribution comes from the northern Barents Sea and the northern Kara Sea.

We note that, while Figure 9 in Steele and Boyd (1998) does indeed illustrate salty shelf waters advected from both the Barents and Kara Seas, in the text they write that, "The only salty (i.e., S > 33) shelf sea in the eastern longitudes of the Arctic Ocean is the Barents Sea, which led *Aagaard et al.* [1981] to speculate that this would be the most likely source of CHL formation via the mechanism show in Figure 2a."

We have included both the Kara and Barents Seas as possible sources of relatively salty shelf water in our discussion of Steele and Boyd's mechanism but note that the Barents Sea is likely the primary source.

The text has been corrected and expanded in the revised manuscript (between Page 2, Line 29 and Page 3, Line 4) to offer a better description of the "advective-convective" mechanism described in Steele and Boyd (1998).

Page 2, lines 13-16: The description of the process proposed by Kikuchi et al. (2004) cannot be correct. Freezing on the Atlantic water at its entrance, should that be possible, would lead to convection and homogenization of the Atlantic layer and perhaps convection to the bottom. A low salinity upper layer must exist for this mechanism to work, creating the bent TS curves.

We have removed the lines referring to the Kikuchi et al. (2004) paper to avoid further confusion. The "ideal" situation introduced by Kikuchi et al. is not mentioned further in the manuscript and not relevant to the discussion.

Page 2, lines 18-23: Rudels et al. (2004) claim that the water from the Barents Sea that eventually contributes to the Barents Sea branch halocline water also is formed by sea ice melting on Atlantic water. The higher salinity compared to the Fram Strait branch halocline water is due to the lower temperature of the Atlantic water when it encounters the sea ice in the eastern Barents Sea.

We have added statements pointing out this distinction on Page 3, Lines 23-26 of the revised manuscript.

Page 2, line 29: The Barents Sea branch halocline is initially more saline and eventually it also becomes warmer and thicker due to mixing with underlying Atlantic water.

We have added statements pointing out this distinction on Page 3, Lines 23-26 of the revised manuscript.

Page 4, first paragraph: There is no halocline water mass in the Nansen Basin west of Severnaya Zemlya and the thermocline and halocline coincide.

This paragraph refers to the study area as a whole and indicates a weak or absent halocline. We later argue that there exists a seasonal halocline (previously described by Rudels et al., 1996 and Steele & Boyd, 1998) that is distinct from a permanent halocline. This seasonal halocline temporarily separates the surface mixed layer from the thermocline but is eroded during winter mixing until additional stratification (supplied by relatively fresh Siberian shelf waters) restricts this mixing to shallower layers. The seasonal halocline transitions to a more permanent halocline across the front observed north of Severnaya Zemlya.

Sections 4.1 and 4.2 have been expanded in the revised manuscript and further clarify this distinction (e.g., Page 8, Lines 11-13).

Page 4, line 9: In the supplementary material the depth of the winter mixed layer with salinity >34 ranges between 30m to 94m (L1) and between 42m and 58m (L2). Most of the depths were larger than 50m. (There were also two stations with depths close to 200m on L2 but the temperatures were close to 0C and the salinities >34.8. Should these observations be correct we would have winter mixing into the Atlantic water. This shows that the temperature minimum as a limit for winter convection should be used with care. However, in general it underestimates the winter mixed layer depth.)

The stations exhibiting deeper winter mixed layers were located on the shelf (water depths $\leq$ 500 m) and were associated with cold and relatively homogeneous bottom layers as well as maximum Atlantic layer temperatures of < 0.5°C. We have added text to the table caption in the Supplementary Materials discussing potential errors in the assignment of winter mixed layer depths based upon this method. We have also visually inspected all of the potential temperature profiles and have removed WML depths from the table that either appear to be in error or seem ambiguous. We also note that these removals do not largely alter the mean WML depth or

salinity and therefore do not greatly impact our subsequent calculations or associated interpretations.

Page 5, lines 19-21: Freezing shifts the mixing line between Atlantic water and meteoric water to the right, making it steeper. The Laptev Sea shelf input would then contain more brine than the East Siberian Sea input.

That is correct. The overall dominance of brine over sea ice melt (i.e., net ice formation) in the Laptev Sea and the higher contribution of sea-ice meltwater in the East Siberian Sea versus the Laptev Sea have been documented in previous studies (e.g., Bauch et al., 2011; 2013; Anderson et al., 2013).

Text explaining the impact of ice formation on salinity and d18O has been added to the revised manuscript on Page 6, Lines 25-32.

We have also included citations to Bauch et al. (2011; 2013) and Anderson et al. (2013) on Page 7, Lines 9-15.

Page 5, last paragraph: Here I am not sure that I follow the authors thinking. As the water from the Nansen Basin (the sea ice melt water branch) becomes covered by les saline shelf water with larger content of meteoric water, vertical mixing with the overlying water will lead to a mixing line with the observed slope. However, the bulk of the halocline water mass is derived from the winter mixed layer advected towards the Laptev Sea. The mixing changes slightly the properties of the halocline, but it does not provide any significant volume. Is this what the authors mean, or do they claim that here exits a major different source of the halocline water containing initially more meteoric water?

We are not claiming that there exists a different source of halocline water. The reviewer's first interpretation is correct. Mixing with overlying, less saline waters results in small changes to salinity and d18O; however, these small changes initiate a movement from the SIM mixing relationship (prevalent on the western side of the defined front) to the MW mixing relationship (prevalent on the eastern side of the defined front) in salinity-d18O space that also corresponds with the migration of the θ-S "kink" (or "bend") that has typically been used to identify lower halocline water. This is the first step in the process that transforms the seasonal halocline into the permanent halocline and begins to form the cold halocline layer.

We have significantly expanded the text of sections 4.1 and 4.2 in the revised manuscript to clarify these points (e.g., Page 8, Lines 14-31).

Page 6, lines 10-14: Once the low salinity polar mixed layer is formed, any shelf contribution having higher salinity than the polar mixed layer will contribute to the halocline. The question is, how large are these contributions compared with the initial Fram Strait branch and Barents Sea branch contributions?

The reviewer makes an excellent point and we certainly agree that any shelf contribution with a salinity exceeding that of the freshened polar mixed layer will contribute to the halocline. Our observations suggest that the majority of these shelf contributions will occur eastward of the observed front north of Severnaya Zemlya and that initial contributions serve to cap LHW (establishing a permanent halocline) and further contributions will build the cold halocline layer. Thus, we argue LHW ($34.2 \leq S \leq 34.5$) is primarily "*basin-derived*" and the capping of this water mass by Siberian shelf waters both isolates LHW (completing the formation mechanism) and in so doing, forms the cold halocline layer. The majority of shelf waters contributing to the halocline will have a salinity < 34.2 and therefore contribute to the "lower MW mixing branch" defined in this study. While there are certainly exceptions, such as more saline waters formed in polynyas, we suggest that the mechanisms we describe are responsible for the bulk of halocline layer formation. We have noted in this paragraph that this hypothesis does not agree with the circulation scheme recently proposed by Bauch et al. (2016).

We have added text to the revised manuscript (Page 9, Lines 18-23) to clarify these points.

Page 6, lines 26-28: This description is essentially correct, but why not state explicitly that to create an halocline water mass from the winter mixed layer, this layer has to be capped by a water mass with lower salinity advected from the Laptev Sea shelf?

We have made this statement in the revised manuscript as suggested by the reviewer on Page 8, Lines 10-11.

Page 6, lines 30-32, Page 7, lines 1-5: These mixing examples are interesting, but I think that it would be simpler to think of the winter mixed layer being capped by low salinity water. The initial thermostad and halostad would then be freshened by mixing with the low salinity layer above and heated and become more saline by mixing with the Atlantic water below. This would create the vertical gradients in temperature and salinity that characterize the halocline. Furthermore, I thought that freezing does not fractionate the oxygen isotopes. Brine rejection would then not change the oxygen-18 value. What is the reference for the adopted slope? On page 8, line 13 brine rejection is characterized as "negative sea ice melt". Would that not give a slope that increases the delta-oxygen-18 value as well as the salinity?

We included this simple mixing scenario to further test the possibility of our proposed mechanism to explain both the d18O and potential temperature observations in the LHW. While we do not claim that this simple mixing is necessarily responsible for the observed halocline water properties, we note that such mixing can explain our observations.

We make this statement in the revised manuscript on Page 9, Lines 12-14.

Ice formation (freezing) results in the rejection of salts from the sea ice matrix as well as a preferential rejection of 16O (the lighter isotope). As a result brine is characterized by higher salinities and a more negative d18O value whereas sea ice (and therefore sea ice meltwater) is characterized by a somewhat more positive d18O value. This fractionation is not large; fractionation factors range between about 1.6 and 2.8 ‰ depending upon the age of the ice and the rate of freezing (Eicken et al., 1998; Macdonald et al., 1995; Melling and Moore, 1995), but it does result in a steeper salinity-d18O slope (as illustrated in Fig. 5e of the revised manuscript).

Text has been added on Page 6, Lines 25-32 clarifying this point.

Page 7, lines 6-7: To me the lower halocline water and the cold halocline layer are the same, at least in this location. Once we enter the Canada Basin with Pacific inflow through Bering Strait the situation is different.

We somewhat disagree. We have argued in the introduction that the lower halocline water is a separate water mass that essentially marks the base of the cold halocline layer (formed from mixing and additional inputs from the shelves) and represents a transition between the halocline and reverse thermocline.

Also, see our response to the comment regarding Page 6, lines 10-14.

Page 7, lines 23-24: I agree with this statement.

Excellent.

Page 8, lines 10-11: Why does the delta-oxygen-18 decreases? A reference is needed.

The d18O decreases (along with salinity) because these waters mix with overlying waters characterized by lower salinities and lower d18O values, due to the influence from both river runoff (characterized by d18O values < -18 ‰) and brine (highly negative d18O values). We have referred to Fig. 5e at the end of this sentence in the revised manuscript (Page 11, Line 15) to illustrate these changes.

We also note that a full description of the changes in d18O due to mixing with MW and ice formation, complete with references, has been added in response to a previous comment (see Page 6, Lines 25-32 of the revised manuscript).

Page 8, lines 17-21: Does this mean that there are two separate branches of halocline water, or only that when the Fram Strait and the Barents branches cross the front, their upper parts are changed from being homogenized by brine rejection and convection to evolve by mixing with overlying low salinity and underlying Atlantic water?

We argue that the majority of our observations describe the formation and modification of a single source of lower halocline water (basin-derived or Fram

Strait branch LHW) but note that we only glimpsed influences from Barents Sea Branch halocline water.

We have added text throughout the manuscript, but particularly on Page 11, Lines 9-10, pointing out this distinction.

We suggest, like Rudels et al. (1996), that the Fram Strait branch halocline water is changed from a seasonal halocline to a permanent halocline after crossing the Severnaya Zemlya front. The salinity-d18O characteristics are altered (transition from SIM to MW mixing branch) due to homogenization and ice formation and then the LHW is capped by Siberian shelf water east of the front, making the halocline permanent and building up the cold halocline layer.

We have also noted that this scheme contrasts with that recently published by Bauch et al. (2016).

Figure 1: I would have appreciated to see not only TS curves but also profiles from the different sections.

Figure 1 is rather large and we do not discuss features of the individual salinity and temperature profiles in the text. Instead, we have relied primarily on descriptions in θ-S space. While we do not agree that these profiles are needed in the main text, we have included two additional figures in the Supplementary Materials that show potential temperature and salinity profiles from selected stations along each transect so other interested readers may view them as desired.

Summary: My concern about this manuscript should be clear after the comments above. If the authors mean that there are two distinct branches, one sea ice melt branch and one meteoric water branch, they have to argue their case better. If it is only a transition between the two branches across the front, the manuscript does not bring much new information. However, the use of the oxygen-18 data is interesting, but some of the adopted slopes have to be explained better.

As stated in our responses above, we do not argue for two distinct branches but instead offer geochemical evidence from salinity and stable oxygen isotope mixing relationships to support a single mechanism that describes the transition from a seasonal to permanent halocline layer, in general agreement with the mechanism proposed by Rudels et al. (1996). While this evidence does not necessarily offer up a new mechanism by which to classify halocline water formation it does offer geochemical data that agrees with hypotheses based primarily on interpretations of θ-S data. We note that our conclusions also disagree with recent work published by Bauch et al. (2016) supporting distinct sources of lower halocline water from the Kara Sea shelf. Finally, the salinity-d18O mixing regimes presented in this study may be used in future studies to evaluate subsequent mixing and modification to the halocline layer. The apparent robust nature of these mixing regimes suggests that the "convective mechanism" of LHW formation has been more-or-less consistent

despite variations in the distribution and strength of the halocline layer. We argue that the stability of these relationships may make them suitable for the evaluation of modifications to the halocline due to mixing and/or interactions with shelf sediments that increase nutrient concentrations and decrease dissolved oxygen concentrations.

The manuscript might be published after major revisions, some based on my comments given above.

Based on the comments provided by the two reviewers, we have made major revisions that have improved the quality and clarity of the manuscript.

Combining physical and geochemical methods to investigate lower halocline water formation and modification along the Siberian continental slope

Matthew B. Alkire[1], Igor Polyakov[2], Robert Rember[2], Andrey Pnyushkov[2], Vladimir Ivanov[3, 2], Igor Ashik[3]

[1]Applied Physics Laboratory, University of Washington, Seattle, WA USA
[2]International Arctic Research Center, University of Alaska Fairbanks, Fairbanks, AK USA
[3]Arctic and Antarctic Research Institute, St. Petersburg, RUS

Correspondence to: Matthew B. Alkire (malkire@apl.washington.edu)

Abstract. A series of cross-slope transects were occupied in 2013 and 2015 that extended eastward from St. Anna Trough to the Lomonosov Ridge. High-resolution physical and chemical observations collected along these transects revealed fronts in the potential temperature and the stable oxygen isotopic ratio ($\delta^{18}O$) that were observed north of Severnaya Zemlya (SZ). Using linear regressions, we describe mixing regimes on either side of the front that characterize a transition from a seasonal halocline to a permanent halocline. This transition describes the formation of lower halocline water (LHW) and the cold halocline layer via a mechanism that has been previously postulated by Rudels et al. (1996). Initial freshening of Atlantic water by sea-ice meltwater occurs west of SZ whereas higher influences of meteoric water and brine result in a transition to a separate mixing regime that alters LHW through mixing with overlying waters and shifts the characteristic temperature-salinity bend from higher ($34.4 \leq S \leq 34.5$) toward lower ($34.2 \leq S \leq 34.3$) salinities. These mixing regimes appear to have been robust since at least 2000.

1 Introduction

The role and relative importance of Atlantic water (AW) heat in shaping the Arctic Ocean's ice cover is still under debate (e.g., Polyakov et al., 2012b). One significant source of uncertainty is the impact of diapycnal fluxes on the cold halocline layer (CHL), which separates the fresh and cold surface mixed layer (SML) from the warmer and saltier AW (e.g., Aagaard et al. 1981; Pfirman et al. 1994; Schauer et al. 1997; 2002). The stratification of the CHL, representing strong vertical gradients of salinity and density though a negligible gradient of temperature (resulting in a relatively weak θ-S slope), impedes vertical mixing and upward transport of AW heat (e.g., Rudels et al., 1996; Steele & Boyd, 1998). Underlying the halocline is the reverse thermocline, wherein the temperature increases with depth toward the core of the AW (150-400 m), resulting in a steeper θ-S slope relative to the halocline layer. The LHW is a distinct water mass that is commonly identified

Matthew Alkire 9/1/17 10:22 AM
Deleted: convective

Matthew Alkire 9/11/17 12:40 PM
Formatted: Tabs: 1.69", Left

Matthew Alkire 9/1/17 10:32 AM
Formatted: Font:Symbol

Matthew Alkire 9/1/17 10:29 AM
Deleted: The base of the CHL represents a transition between the halocline

Microsoft Office User 9/19/17 1:32 PM
Deleted: l

Matthew Alkire 9/11/17 12:28 PM
Deleted: and

Matthew Alkire 9/11/17 12:28 PM
Deleted: This transition is known as the

Matthew Alkire 9/1/17 3:04 PM
Deleted: ,

Matthew Alkire 9/1/17 3:10 PM
Deleted: separate

Matthew Alkire 9/1/17 10:30 AM
Formatted: Font:Symbol

by a "kink" in the θ-S diagram (see Fig. 1c) and forms the base of the CHL; as such, the LHW represents a transition between the halocline and reverse thermocline layers. The LHW was first identified as a separate water mass by Jones and Anderson (1986). They pointed out that the nutrient concentrations were significantly lower than those characterizing the comparatively nutrient-replete upper halocline water of Pacific origin. These differences were further highlighted by the NO parameter, defined as $NO = 9*[NO_3^-] + [O_2]$, as the LHW was characterized by a local minimum whereas the upper halocline was characterized by a local maximum. We note that some studies interchange the CHL and the LHW. However, we offer the following distinction. While the CHL and LHW may share similar origins/formation mechanisms, we argue that the LHW ($34 \leq S < 34.5$) is a comparatively less modified and distinct water mass compared to the CHL ($33 < S < 34$) that receives inflows from surrounding shelves and is more heavily modified through mixing with overlying waters. The formation of LHW and its modification through diapycnal and/or turbulent mixing with underlying Atlantic water on the Siberian continental slope have important implications for the heat budget and sea ice cover of the Arctic Ocean (e.g., Polyakov et al., 2017). Therefore, it is important to be able to discern between LHW varieties formed by different mechanisms and the modification of these LHW sources through mixing.

Various mechanisms have been proposed for explaining the formation of LHW in the Nansen Basin of the Arctic Ocean. Initially, hypotheses suggested LHW was formed via salinization of Siberian shelf waters through brine rejection and subsequent transport of these waters offshore (Aagaard et al., 1981; Jones & Anderson, 1986; Steele et al., 1995). Such hypotheses have been previously referred to as the "*advective mechanism*" of LHW formation in the literature due to its formation entirely on the shelves and subsequent advection into the deep basins. At present, it is generally agreed that the primary mechanism of LHW formation results from the modification of AW by melting sea ice upon entry into the Arctic through Fram Strait and the Barents Sea (Rudels et al., 1996; 2004). In this scenario, relatively fresh ($34 \leq S \leq 34.3$) SML water undergoes convective mixing through cooling and brine release during winter sea ice formation. This winter mixed layer (WML) is advected along the Siberian continental margin and is eventually capped by low-salinity shelf waters moving offshore, limiting the depth of subsequent convection. This hypothesis has been typically referred to as the "*convective mechanism*" of LHW formation in the literature. We point out that the "*advective*" and "*convective*" labels for differentiating LHW formation are misleading, particularly since the latter mechanism depends upon the advection of the WML eastward along the slope until low-salinity shelf waters are advected offshore and increase the stratification. Convective and advective processes are involved in both formation mechanisms; therefore, we have chosen to replace these terms with "*basin-derived*" and "*shelf-derived*", respectively, to minimize further confusion.

Steele and Boyd (1998) suggested an "*advective-convective mechanism*" wherein the CHL/LHW is derived from both salty shelf waters originating from the Kara and (primarily) Barents Seas (i.e., "*shelf-derived*") and the WML of the deep Nansen Basin where convective mixing homogenizes surface waters that have been previously freshened by sea ice meltwater (*"basin-derived"*). The salty shelf waters advect northward into either a winter mixed layer (100-150 m thick) of similar salinity (S~34) or below a summer mixed layer and into a seasonal halocline layer that will be eroded during convective mixing the following winter. This combined mixed layer will eventually progress eastward where fresher shelf

Matthew Alkire 9/1/17 10:49 AM
Deleted:

Matthew Alkire 8/2/17 7:44 PM
Deleted: 1

Matthew Alkire 9/1/17 11:02 AM
Formatted: Subscript

Matthew Alkire 9/1/17 11:02 AM
Formatted: Superscript

Matthew Alkire 9/1/17 11:02 AM
Formatted: Subscript

Matthew Alkire 9/1/17 3:14 PM
Formatted: Underline

Matthew Alkire 9/1/17 3:14 PM
Formatted: Underline

Matthew Alkire 9/11/17 12:42 PM
Deleted:

Matthew Alkire 9/1/17 11:12 AM
Deleted: (i.e., the *advective mechanism*)

Matthew Alkire 9/1/17 11:11 AM
Formatted: Font:Italic

Matthew Alkire 9/1/17 11:12 AM
Deleted:

Matthew Alkire 9/1/17 11:14 AM
Formatted: Font:Italic

Matthew Alkire 9/1/17 11:16 AM
Formatted: Font:Italic

Matthew Alkire 9/1/17 11:16 AM
Formatted: Font:Italic

Matthew Alkire 9/1/17 11:15 AM
Deleted:

Matthew Alkire 9/1/17 2:50 PM
Formatted: Font:Italic

Matthew Alkire 9/1/17 2:36 PM
Deleted: combined,

Matthew Alkire 9/1/17 11:20 AM
Formatted: Font:Italic

Matthew Alkire 9/1/17 2:36 PM
Deleted: LHW

Matthew Alkire 9/1/17 2:40 PM
Deleted: formed primarily in the marginal ice zone north of the Barents Sea via convective processes and subsequently interleaves between the WML and AW, forming the CHL through mixing during advection.

Matthew Alkire 9/1/17 2:50 PM
Formatted: Font:Italic

waters from the eastern Kara and Laptev Seas will mix into surface and near-surface waters, providing the necessary stratification to cap the LHW against deeper convective mixing and form a permanent halocline layer. In our view, the "capping" process is primarily responsible for the formation of the CHL atop the LHW that is formed by either *shelf-derived* and/or *basin-derived* processes. Rudels et al. (2004) also suggested that both mechanisms of halocline formation (i.e., *shelf-* and *basin*-derived) are possible, resulting in two different sources of halocline water in the eastern Arctic: Fram Strait Branch (FSB) and Barents Sea Branch (BSB) halocline waters. According to Rudels et al. (2004), the FSB branch variety of halocline water is formed via interaction between inflowing AW and sea ice north of Svalbard and subsequent convection in the Nansen Basin, quite similar to the *basin-derived LHW* of Rudels et al. (1996). The BSB variety is formed in the Barents Sea through a complex combination of processes (including cooling, melting sea ice, mixing with freshwater from the Norwegian Coastal Current, net precipitation, river runoff from the Kara Sea, and brine release during ice formation, though the latter process is thought to be a less likely component) resembling the mechanism outlined by Steele & Boyd (1998). Rudels et al. (2004) further postulates that after entering the Eurasian Basin through St. Anna Trough (SAT), the BSB halocline water remains close to the Siberian continental slope, and after crossing the Lomonosov Ridge ventilates the lower halocline of the Makarov Basin between the Mendeleyev Ridge and the Chukchi Cap as well as the southern Canada Basin. In contrast, the FSB halocline water is displaced farther offshore, ventilating the halocline of the Amundsen and Makarov Basins, as well as northern Canada Basin.

The BSB halocline water has been found to be saltier, thicker, and warmer compared to colder and fresher FSB halocline waters. These distinctions can be visually recognized in a θ-S diagram: the cooler FSB variety is expected to exhibit a sharp θ-S kink close to the freezing point whereas the warmer BSB variety is generally characterized by a smoother kink farther from the freezing point line. Thus, differences can be observed in the properties of halocline waters occupying the slope ("on-slope") versus those located farther offshore ("off-slope"). Woodgate et al. (2001) attributed these cross-slope distinctions to differences in the formation processes (i.e., *shelf-* vs. *basin*-derived halocline water). Rudels et al. (2004) attributed the higher salinity of the BSB halocline water to lower Atlantic water temperatures in the Barents Sea since cooler waters will melt less ice. The higher temperature of BSB halocline water was attributed to enhanced turbulent mixing between the BSB halocline water and underlying (and warm) AW as they are advected eastward along the Siberian slope. They argued that the mixing acts to entrain more AW into the halocline, making it both thicker and warmer while simultaneously cooling the AW layer. Dmitrenko et al. (2011) argued that turbulent vertical mixing occurring locally on the Laptev Sea slope explains the differences observed between warmer/on-slope and cooler/off-slope LHW properties observed along a regularly occupied section (~126 °E) in the Laptev Sea between 2002 and 2009; however, they did not consider the possibility of lateral advection of cross-slope differences from upstream.

Despite the importance of river water and sea-ice melt/brine in LHW formation, few studies have utilized $\delta^{18}O$ to investigate the formation or modification of LHW through mixing. It is the purpose of this paper to pair a high density of $\delta^{18}O$ measurements (focused on the halocline layer) with CTD-based temperature and salinity measurements collected along

Matthew Alkire 9/11/17 1:01 PM
Formatted ... [1]
Matthew Alkire 9/1/17 2:37 PM
Deleted: In contrast, Kikuchi et al. (2004) ... [2]
Matthew Alkire 9/11/17 1:01 PM
Formatted ... [3]
Matthew Alkire 9/1/17 2:54 PM
Formatted ... [4]
Matthew Alkire 9/1/17 2:54 PM
Formatted ... [5]
Matthew Alkire 9/1/17 2:55 PM
Deleted: *convective LHW mechanism*
Matthew Alkire 9/1/17 11:59 AM
Formatted ... [6]
Matthew Alkire 9/1/17 12:13 PM
Formatted ... [7]
Matthew Alkire 9/1/17 12:12 PM
Deleted:
Matthew Alkire 9/1/17 2:55 PM
Deleted: advective-convective mechanism
Matthew Alkire 9/11/17 2:03 PM
Formatted ... [8]
Matthew Alkire 9/20/17 8:07 PM
Deleted: ,
Matthew Alkire 9/20/17 8:07 PM
Deleted: ,
Matthew Alkire 9/1/17 2:59 PM
Deleted: both
Matthew Alkire 9/20/17 10:32 AM
Deleted: (e.g., Fig 1e)
Matthew Alkire 9/1/17 3:00 PM
Deleted: thicker and
Matthew Alkire 9/20/17 10:32 AM
Deleted: (e.g., Fig. 1k)
Matthew Alkire 9/1/17 3:00 PM
Deleted: *advective*
Matthew Alkire 9/1/17 3:00 PM
Formatted ... [9]
Matthew Alkire 9/1/17 3:00 PM
Deleted: *convective*
Matthew Alkire 9/1/17 3:00 PM
Formatted ... [10]
Matthew Alkire 9/1/17 12:03 PM
Deleted: these differences
Matthew Alkire 8/2/17 10:10 AM
Deleted: halocline water

a series of cross-slope transects extending from the SAT to the Lomonosov Ridge to improve our understanding of LHW formation, circulation, and modification through mixing with Siberian shelf waters and underlying AW.

2 Data & methods

In collaboration with the Arctic and Antarctic Research Institute (St. Petersburg, Russia), oceanographic cruises were conducted within the Eurasian Basin and along the slope of the Kara, Laptev, and East Siberian Seas during summers of 2013 (August 23-September 19) and 2015 (August 28-September 26) aboard the research vessels *Akademik Fedorov* and *Akademik Tryoshnikov*, respectively (Fig. 2). Totals of 116 (2013) and 94 (2015) hydrographic stations were occupied during the cruises. At all stations, a rosette equipped with 24 Niskin bottles, a Seabird SBE9*plus* CTD (conductivity-temperature-depth), and additional sensors were deployed (further details provided in Supplementary Text S1). At all but 8 (2013) and 6 (2015) stations, water samples were collected for a variety of chemical and biological measurements at routine depths of 500, 250, 200, 150, 140, 130, 120, 110, 100, 90, 80, 70, 60, 50, 40, 30, 20, 10, and 2-4 m (surface).

Samples for $\delta^{18}O$ analyses were collected into 20 mL glass vials, the caps of which were fitted with conical polyethylene inserts, parafilmed, and shipped to the Stable Isotope Laboratory, Oregon State University, for analysis via the CO_2 equilibration method on a Finnegan Mat 251 mass spectrometer. Totals of 1254 and 1940 samples were collected in 2013 and 2015, respectively. Precision was estimated to be ± 0.02 ‰ (2013) and 0.04 ‰ (2015), based on the mean standard deviations of field duplicates. Laboratory duplicates were also conducted to ascertain the performance of the mass spectrometer. Of these, the mean standard deviation was ± 0.02 ‰ during both years. Bottle salinities are not reported due to malfunction of the salinometer available aboard each ship. Instead, CTD properties were matched to bottles via averaging measurements associated with each bottle trip depth using the bottle (.ros) files recorded for each cast. The accuracy of temperature and conductivity measurements recorded by the CTD is expected to be within ± 0.001°C and ± 0.0003 S m^{-1}, respectively, per manufacturer specifications. For further details and data access, readers are referred to the Supplementary Materials, NABOS project website (http://research.iarc.uaf.edu/NABOS2/), and the NSF Arctic Data Center (https://arcticdata.io).

3 Results

Transects occupied during 2013 indicated that the base of the WML, identified as a potential temperature minimum (θ_{min}) below the warmer and fresher SML (Rudels et al., 1996), was associated with salinities > 34. The presence of a seasonal, rather than a permanent, halocline layer was evidenced by relatively weak stratification between the base of the WML and the θ-S bend identifying LHW (Fig. 3), potential temperatures near the freezing point at S = 34.1 (e.g., red lines in Fig. 3d), and higher salinities (S ≥ 34) at 40-50 m depth (Fig. 4d); thus, a permanent halocline was either very weak or absent throughout most of our study area (Steele and Boyd, 1998; Kikuchi et al., 2004; Bourgain and Gascard, 2011).

Matthew Alkire 8/2/17 7:46 PM
Formatted: Font:Not Bold, Not Italic

Matthew Alkire 8/2/17 10:11 AM
Deleted: and ± 0.001C

Matthew Alkire 8/2/17 10:11 AM
Deleted: /or

Matthew Alkire 8/2/17 7:47 PM
Deleted: 2

Matthew Alkire 9/20/17 10:38 AM
Deleted: , potential temperatures near the freezing point at S = 34.1 (e.g., red lines in Fig. 1e), and

Matthew Alkire 9/20/17 10:38 AM
Deleted: relatively weak stratification between the base of the WML and the θ-S bend identifying LHW (Fig. 1);

Matthew Alkire 9/20/17 10:38 AM
Deleted: CHL

At stations in the western part of the study area, it was also apparent that the θ-S kink was sharp, close to the freezing point, and at a relatively shallow depth (typically ≤ 50 m) (Fig. 3a-c) indicating that the halocline was *basin-derived* and likely seasonal (Steele et al., 1995; Rudels et al., 1996; Steele and Boyd, 1998). Farther eastward, the L3 and L4 transects exhibited a front that separated stations closer to shore versus those farther offshore (Fig 3d-e). This front marked a significant change in the core AW temperature (Fig. 4f) as well as a θ increase (Fig. 4e) and $\delta^{18}O$ decrease (Fig. 4c) in the salinity range 34.4 ≤ S ≤ 34.5 and an apparent shift of the θ-S bend marking the position of LHW towards lower salinities (34.2 ≤ S ≤ 34.3) (e.g., Fig. 3d). Coincident with this θ-S front, there was also a change in the predominant source of freshwater near the surface. Sea-ice meltwater (SIM) fractions were positive and larger than fractions of meteoric water (MW) along the lengths of sections SAT, L1, and L2 as well as the nearshore stations comprising sections L3 and L4; however, transects L5, L5.5, and L6 all exhibited predominate freshening by MW (Fig. 4a-b). Bauch et al. (2014) reported a similar, zonal gradient along the Siberian slope, with increasing contributions of both MW and brine from west to east, where shelf waters are advected offshore at ~140 °E (in the northeastern Laptev Sea) and contribute to layers overlying LHW (S ≤ 33).

The easternmost stations of the SAT transect and the southernmost stations of transects L2 and L3 exhibited θ-S characteristics expected for BSB AW (black lines in Fig. 3a, c, d). At L5, three stations inshore of the ~1250 m isobath (< 77.2 °N) exhibited θ-S characteristics (Fig. 3f) synonymous with northern Barents Sea Shelf Water (Woodgate et al., 2001). These observations generally agree with the expectation that BSB waters are restricted to the slope and indicate that the predominance of FSB (or *basin-derived*) LHW throughout most of the study area. We note that the θ-S characteristics of BSB waters were not apparent along transects L1 or L4, possibly indicating that we failed to sample far enough inshore to capture BSB waters at these transects.

Matthew Alkire 8/2/17 7:47 PM
Deleted: 1…d…f ... [11]

Matthew Alkire 9/11/17 7:41 PM
Deleted: *convectively formed*…1…g…h…2…2…2…1…g…2 ... [12]

Matthew Alkire 9/11/17 7:41 PM
Formatted: Font:Italic

Matthew Alkire 8/2/17 7:48 PM
Deleted: 1…d…f…g…1…i…/ ... [13]

Matthew Alkire 9/11/17 7:43 PM
Formatted: Font:Italic

Matthew Alkire 9/11/17 7:43 PM
Deleted: *convective*

4 Discussion

4.1 Geochemical separation of mixing regimes

The coincident shift in freshwater sources was also marked by an obvious change (or "break") in the $\delta^{18}O$-S slope at 34.4 ≤ S ≤ 34.5 (Fig. 5a). A change in $\delta^{18}O$-S slope may indicate a change in the mixing regime that typically involves the introduction of a new water mass. For example, on the western side of the front, the salinity-$\delta^{18}O$ data may be explained by simple mixing between the Atlantic layer and a SML that is freshened predominately by SIM. The change in $\delta^{18}O$-S slope at the front indicates the introduction of MW as the primary source of freshwater (Fig. 4a-b). However, it is unclear from the data presented in Fig. 5a whether or not mixing of MW is restricted to shallower depths (associated with salinities < 34.5;

Matthew Alkire 9/12/17 11:19 AM
Deleted: break…mixing …3 ... [14]

i.e., "below" the slope break) or if this new mixing regime extends over the full salinity range (i.e., both "above" and "below" the slope break). Therefore, we explore this change in mixing in more detail by comparing simple, linear regressions of salinity and $\delta^{18}O$. At each transect, two groups of regressions were assessed. The first group included data at salinities ($S \geq 34.5$) "above" the slope break. The second group included data at salinities "below" the slope break ($34 \leq S < 34.5$).

First, we report results of the linear regressions encompassing data above the slope break ($S \geq 34.5$). The stations occupied along the SAT, L1, L2, and southern portions of the L3 and L4 transects (including those stations exhibiting BSB influence) all exhibited similar slopes (i.e., linear mixing regimes) in $\delta^{18}O$-S space that indicated predominate freshening by SIM (Table 1). This freshening by SIM was evident by the higher SIM fractions observed at these stations (e.g., Fig. 4b) as well as the range (between -4.7 and -8.9 ‰) of intercepts ($S = 0$) computed from simple, linear regressions of the data (Table 1). Data collected from this group of stations all appeared to plot along a single, linear mixing line at the higher end of the salinity range ($S > 34.5$), just above the observed $\delta^{18}O$-S break. In fact, separate linear regressions from these transects were all statistically indistinguishable (Table 1); thus, a single $\delta^{18}O$-S linear regression was constructed using these data to define what we refer to as the "SIM mixing branch" for $S \geq 34.5$ (Fig. 5b). Similarly, data collected from stations farther offshore on the L3 and L4 transects were combined with those along the L5 transect to construct the "MW mixing branch" for $S \geq 34.5$ (Fig. 5c and Table 1). Notably, the slopes and intercepts characterizing the mixing regimes of the SIM and MW branches were significantly different for $S > 34.5$. This difference indicates that the shift in mixing that occurred across the SZ front was not restricted to lower salinities ($S < 34.5$) but extended to higher salinities.

Next, we report the results of linear regressions conducted on data below the slope break, specifically in the salinity range typically associated with LHW ($34 \leq S < 34.5$). Linear regressions conducted on the stations comprising the SIM branch returned coefficients (Table 2) that were statistically indistinguishable from the more saline ($S > 34.5$) regressions (Table 1); thus, the SIM branch extended over most of the water column at stations west of SZ. In contrast, there were significant changes in the $\delta^{18}O$-S slopes characterizing the stations of the MW branch (Fig. 5c). Linear regressions returned steeper slopes and more negative intercepts that indicated higher influences of both MW and brine (i.e., negative SIM); a situation typical of Laptev Sea shelf waters (Bauch et al, 2011). Net ice formation (freezing) results in the rejection of salts from the sea ice matrix as well as a small, but preferential rejection of ^{16}O over ^{18}O. As a result, brine is characterized by higher salinities and more negative $\delta^{18}O$ values whereas sea ice (and therefore sea ice meltwater) is characterized by lower salinities and somewhat more positive $\delta^{18}O$ values. This fractionation is not large; fractionation factors range between about 1.6 and 2.8 ‰ depending upon the age of the ice and the rate of freezing (Macdonald et al., 1995; Melling and Moore, 1995; Eicken, 1998), but it does deflect a simple, linear mixing line between AW and MW to the right, resulting in a steeper salinity-$\delta^{18}O$ slope (as illustrated in Fig. 5c). Therefore, the change in mixing regime across the SZ front altered the $\delta^{18}O$-S slopes of both

Matthew Alkire 9/12/17 11:29 AM
Formatted ... [15]

Matthew Alkire 9/14/17 10:35 AM
Formatted: Underline

Matthew Alkire 9/11/17 7:49 PM
Deleted: T…all …ted…the upper linear mixing line of the …see Supplementary Table S1…3… 3… ... [16]

Matthew Alkire 9/14/17 11:35 AM
Formatted: Underline

Matthew Alkire 9/14/17 11:34 AM
Deleted:
In addition to the separation of the MW and SIM branches at the $\delta^{18}O$-S break ($34.4 \leq S \leq 34.5$), there was

Matthew Alkire 9/14/17 11:40 AM
Formatted ... [17]

Matthew Alkire 9/12/17 10:35 AM
Deleted: also a clear bend in the $\delta^{18}O$-S relationship at salinities ≤ 34.5 on the MW branch 3…This bend indicates a separate mixing regime that characterizes waters overlying the LHW. A l…restricted to the salinity range $34 \leq S < 34.5$ yielded a…s…Siberian ... [18]

Matthew Alkire 9/11/17 8:09 PM
Formatted ... [19]

the lower (S ≥ 34.5) and upper (34 < S < 34.5) portions of the water column. We will discuss potential mechanisms to explain these changes in section 4.2.

Eastward of ~126 ºE, stations along the L5.5 and L6 transects generally exhibited $\delta^{18}O$ values that were somewhat higher/more positive compared to the linear regression/mixing line defined for the lower salinity range (34 < S < 34.5) of the MW branch (Fig. 5d & Table 2). Thus, this mixing relationship is altered between the Laptev and East Siberian Seas, perhaps due to a larger influence from positive (or less negative) SIM and/or entrainment of thermocline waters containing a larger influence from AW. Rivers flowing into the East Siberian Sea are typically characterized by more negative $\delta^{18}O$ values compared to the Lena, Ob, and Yenisey Rivers (Cooper et al., 2008) so increased MW influence cannot solely explain the more positive $\delta^{18}O$ values. Sea-ice meltwater influences are generally higher/more positive in the East Siberian Sea compared to the Laptev Sea, as the Laptev is characterized by net sea-ice formation over melting (and thus a net negative SIM contribution), even during summer months (Bauch et al. 2011; 2013; Anderson et al., 2013). There are fewer data from the higher salinity range (S ≥ 34.5) to assess differences in $\delta^{18}O$-S slopes between the MW branch and transects L5.5 and L6; however, the available data suggest little-to-no statistically significant differences in the regression coefficients (Table 1), indicating that changes in mixing were likely driven by surface and near-surface mixing (i.e., larger contributions from SIM).

4.2 Interpretation of mixing branches: *basin-derived* vs. *shelf-derived*

Aksenov et al. (2011) describe the Arctic Shelf Break Branch (ASBB) of the Arctic Circumpolar Boundary Current as a narrow current that transports halocline waters from the Barents and Kara Seas northward via the SAT and eastward along the Siberian continental slope over approximately the 1500 m isobath. Their description is similar to the circulation scheme of *shelf-derived* (or BSB) LHW proposed by Rudels et al. (2004). More recently, Bauch et al. (2016) used a combination of geochemical tracers collected across the Siberian continental margin between 2005 and 2009 in a principle components analysis to identify four separate LHW types: c1 (S~33), c2 (S~34), c3 (S~34.2), and c4 (S~34.4). Types c2 and c4 were the most commonly observed, originating at the shelf break north of SZ (type c4) or ~126 °E (type c2) and both extending eastward to at least ~140 °E. Bauch et al. (2016) argued that the regular presence of type c4 LHW north of SZ suggests the Kara Sea as a source of this LHW type. They further postulated that this water leaves the Kara Sea via SAT and/or Voronin Trough and circulates around the slope via the ASBB. Similarly, they argue that type c2 LHW is formed in either the northwestern Laptev Sea or (more likely) in the southeastern Kara Sea and transported to the slope via Vilkitsky Strait.

The description offered by Bauch et al. (2016) for the formation and circulation of LHW types c2 and c4 is also reminiscent of *shelf-derived*, BSB LHW. However, these LHW types are found both on and off the slope, rather than restricted to the continental slope as expected for BSB LHW (Woodgate et al., 2001; Rudels et al., 2004). Bauch et al. (2016) argue that off-slope transport might occur directly or via recirculating waters from the eastern Eurasian Basin (van

Matthew Alkire 9/14/17 11:48 AM
Formatted ... [20]

Matthew Alkire 9/14/17 11:36 AM
Deleted: In contrast, a similar linear regression of the SIM branch stations in this salinity range returned coefficients that were statistically indistinguishable from the more saline (S ≥ 34.5) regression (see Supplementary Table S2); thus, the SIM branch extends over the entire water column.

Matthew Alkire 9/11/17 8:24 PM
Formatted: Font:12 pt, Bold

Matthew Alkire 9/14/17 11:50 AM
Deleted: than …lower …3… ... [21]

Matthew Alkire 9/14/17 11:58 AM
Formatted: Underline

Matthew Alkire 9/14/17 12:00 PM
Deleted: Data collected in the same study area in 2015 suggests a very similar hydrographic setting (i.e., weak/absent CHL with similar cross-slope fronts observed at repeated transects). The salinity-$\delta^{18}O$ data generally agree with the scheme proposed here (see Supplementary Tables S4 & S5) as they plot along the three branches characterized using the 2013 data set (Fig. 4a). Furthermore, data collected from different areas of the eastern and central Arctic (specifically the Siberian shelves and the Nansen, Amundsen, and Makarov Basins) also generally plot along the three mixing lines defined in this s ... [22]

Matthew Alkire 9/20/17 8:20 PM
Deleted: ***convection***

Matthew Alkire 9/20/17 8:28 PM
Formatted: Font:Bold, Italic

Matthew Alkire 9/20/17 8:28 PM
Formatted: Font:Bold, Italic

Matthew Alkire 9/20/17 8:20 PM
Deleted: **advection**

Matthew Alkire 9/18/17 11:16 AM
Deleted: *advective…/…*the … in the data ... [23]

Matthew Alkire 9/18/17 11:16 AM
Deleted: *advective*

Matthew Alkire 9/18/17 11:17 AM
Formatted: Font:Italic

Matthew Alkire 9/18/17 11:17 AM
Formatted: Font:Italic

Matthew Alkire 9/15/17 12:53 PM
Deleted: *advective*

Microsoft Office User 9/19/17 3:22 PM
Deleted: /

Matthew Alkire 9/15/17 12:54 PM
Formatted: Font:Italic

der Loeff et al., 2012). We observed θ and $\delta^{18}O$ characteristics associated with salinities of 34, 34.2, and 34.4 that are quite similar to the LHW types described by Bauch et al. (2016); however, these similarities were restricted to MW branch stations located offshore of the continental slope. In addition, the $\delta^{18}O$ values associated with salinities 34.4-34.5 at SIM branch stations were much higher than those reported by Bauch et al. (2016). These apparent discrepancies suggest different formation and/or circulation schemes compared to those provided by Bauch et al. (2016). Here, we offer an alternative hypothesis.

The WML observed at stations located in the western transects (SAT, L1, and L2) is formed through freshening of AW with SIM and some small contribution of MW (likely from net precipitation and runoff entering the Barents Sea) to establish a seasonal halocline; these processes produce the SIM branch. However, this branch only represents an initial condition, as further stratification is necessary to prevent winter mixing from eroding the LHW (i.e., lower salinity waters from the Laptev Sea shelf are needed to "cap" the LHW) and the SIM branch is not observed eastward of SZ. Therefore, the SIM branch is synonymous with the seasonal halocline and the front observed north of SZ marks the start of the transition from the seasonal to the permanent halocline.

We interpret the transition from SIM to MW branches north of SZ as descriptive of the formation of *basin-derived* LHW (Rudels et al., 1996). We suggest that this transformation occurs via homogenization of the upper water column through mixing and salinization from brine expulsion during sea ice formation. To test this hypothesis, we estimated new mixed layer salinities at the SIM branch stations assuming mixing penetrated to the previous WML depth and then calculated the changes in salinity and $\delta^{18}O$ due to sea ice formation. The mean WML depth and salinity was ~50 m and 34.37, respectively, for all SIM branch stations (see Supplementary Table S1). Mixing of the water columns at individual stations down to their respective WMLs resulted in a new, mean mixed layer salinity of ~33.83 with a corresponding $\delta^{18}O$ value of ~0 ‰ (calculated using the SIM branch regression). Too few $\delta^{18}O$ data were collected from the near surface to directly calculate new mixed layer $\delta^{18}O$ values. The use of the SIM branch regression to estimate the new mixed layer $\delta^{18}O$ likely underestimates the influence of MW to the surface layer, particular at the front (sections L3 and L4). As a result, the final $\delta^{18}O$ values computed after sea ice growth are likely biased slightly high/more positive. Brine expulsion from 1.0-1.5 m of sea ice growth increases the salinity to between 34.38 and 34.66 and decreases $\delta^{18}O$ to between -0.05 and -0.08 ‰. These resulting salinity and $\delta^{18}O$ values roughly plot along the upper or lower MW branches (Fig. 5e & Supplementary Figure S1). Therefore, mixing with overlying, less saline waters results in small changes to salinity and $\delta^{18}O$ that are sufficient to initiate a movement from the SIM mixing relationship (prevalent on the western side of the defined front) to the MW mixing relationship (prevalent on the eastern side of the defined front) in salinity-$\delta^{18}O$ space that also corresponds with the migration of the θ-S "kink" (or "bend") that has typically been used to identify LHW. Continued influence from Siberian shelf waters caps the LHW, isolating it from subsequent surface mixing, and results in a break in the $\delta^{18}O$-S slope that

Matthew Alkire 9/18/17 11:19 AM
Deleted: (all … …) ... [24]

Matthew Alkire 9/18/17 11:41 AM
Formatted: Normal, Left, Space Before: 0 pt, After: 0 pt

Matthew Alkire 9/15/17 12:55 PM
Deleted: likely…(…) ... [25]

Matthew Alkire 9/18/17 11:41 AM
Formatted: Font:Not Bold

Matthew Alkire 9/18/17 11:41 AM
Formatted: Font:(Default) Times New Roman, Italic, English (UK)

Matthew Alkire 9/15/17 12:55 PM
Deleted: by convective processes … (ML)…62…22 ... [26]

Matthew Alkire 9/15/17 12:56 PM
Deleted: S3

Matthew Alkire 9/18/17 11:51 AM
Formatted: Font:(Default) Times New Roman, Font color: Auto, English (UK)

Matthew Alkire 9/20/17 10:40 AM
Deleted: ML…79 ... [27]

Matthew Alkire 9/18/17 11:51 AM
Formatted: Font:(Default) Times New Roman, Font color: Auto, English (UK)

Matthew Alkire 9/18/17 1:00 PM
Deleted: d18O

Matthew Alkire 9/18/17 11:51 AM
Formatted: Font:(Default) Times New Roman, Font color: Auto, English (UK)

Matthew Alkire 9/18/17 11:51 AM
Formatted ... [28]

Matthew Alkire 9/15/17 12:57 PM
Deleted:). …25…48 ... [29]

Matthew Alkire 9/18/17 11:52 AM
Deleted: d18O…5…07 ... [30]

Matthew Alkire 9/18/17 11:51 AM
Formatted: Font:(Default) Times New Roman, Font color: Auto, English (UK)

Matthew Alkire 9/18/17 11:52 AM
Deleted: d18O…3 ... [31]

Matthew Alkire 9/18/17 11:51 AM
Formatted ... [32]

Matthew Alkire 9/18/17 11:51 AM
Formatted ... [33]

Matthew Alkire 9/18/17 11:48 AM
Deleted: …results …in the steeper slope ... [34]

defines a shallower mixing regime characterized by a steeper δ^{18}O-S slope and highly negative intercept (i.e., the lower MW branch). We also argue that this latter process is responsible for the formation of the CHL.

While mixing down to the previous year's WML (or shallower) might be expected given the increase in freshwater inventories (and stratification) moving from west to east along the slope, deeper mixing was observed in the study region between 2013 and 2015 (Polyakov et al., 2017). The depth of the 34.4 isohaline ranged between 60 and 100 m at the MW branch stations. If we consider mixing down to 100 m and 1 m of ice formation, the resulting salinity (34.50) and δ^{18}O (0.07 ‰) resemble the upper MW branch at the break point. Thus, both shallower (~60 m) and deeper (~100 m) mixing result in a transition from the SIM branch to the MW branch. Although mixing and brine release can account for salinity and δ^{18}O changes, additional mixing (either lateral or vertical) with warm AW is needed to produce the $\theta \approx -1$ °C that is associated with the LHW of the MW branch. A mixture comprising ~79 % of newly formed MW branch water (34.38, -0.08 ‰, and -1.89 °C) and ~21 % AW (34.9, 0.3 ‰, and 2 °C) would produce the salinity (34.4), θ (-1.07 °C), and δ^{18}O (0 ‰) observed. We have included this simple mixing scenario to further test the possibility of our proposed mechanism to explain both the δ^{18}O and potential temperature observations in the LHW. While we do not claim that this simple mixing is necessarily responsible for the observed halocline water properties, we note that such mixing can explain our observations.

It is also important to note that MW must have been supplied to the region north of SZ to define the front separating SIM and MW branches. We adopt the suggestion made by Bauch et al. (2016) that waters moving off the shelf in the northeastern Laptev Sea (i.e., along the Lomonosov Ridge) are recirculated westward, except we suggest this recirculation does not necessarily provide four distinct sources of halocline water. Any shelf contribution with a salinity exceeding that of the relatively fresh polar mixed layer will contribute to the halocline. Our observations suggest that the majority of these shelf contributions will occur eastward of the SZ front. We argue that LHW ($34.2 < S < 34.5$) is primarily *basin-derived* and initial shelf water contributions serve to cap LHW (and begin to establish the permanent halocline) whereas further contributions to the halocline will have a salinity < 34.2 and therefore contribute to the "lower MW mixing branch" and build the CHL. In support of this hypothesis, we note that the salinity and δ^{18}O values characterizing the four LHW types defined by Bauch et al. (2016) form a salinity-δ^{18}O mixing line ($\delta^{18}O = 0.9828S - 33.901$) similar to the lower MW branch identified in this study (Supplementary Figure S2). This could indicate that the four LHW types described by Bauch et al. (2016) are actually mixtures of *basin-derived* LHW and increasing contributions of MW progressing eastward from SZ.

4.3 Stability of δ^{18}O-S mixing regimes

Using salinity and δ^{18}O observations, we have outlined a hypothesis to describe the transition from a seasonal halocline, formed due to mixing between AW and SIM west of SZ, to a permanent halocline involving winter mixing, ice formation, and the introduction of Siberian shelf waters characterized by high influences of MW and brine east of SZ that largely follows the hypothesis previously described by Rudels et al. (1996). However, we have thus far relied upon data collected

Matthew Alkire 9/18/17 11:50 AM
Deleted: ; …his …also forms ... [35]

Matthew Alkire 9/5/17 9:09 PM
Deleted: 75 …25…05 …88 …25 … observed…0…91 ... [36]

Matthew Alkire 9/15/17 1:41 PM
Formatted ... [37]

Matthew Alkire 9/15/17 1:41 PM
Deleted:

Matthew Alkire 9/18/17 12:01 PM
Formatted ... [38]

Matthew Alkire 9/18/17 11:56 AM
Deleted: extend to halocline waters but instead only to near surface waters containing MW and brine.

Matthew Alkire 9/15/17 1:05 PM
Deleted: *convectively formed*

Matthew Alkire 9/15/17 1:06 PM
Formatted: Font:(Default) Times New Roman, Italic, English (UK)

Matthew Alkire 9/14/17 12:00 PM
Formatted ... [39]

Matthew Alkire 9/18/17 12:12 PM
Formatted: Font:(Default) Symbol, English (UK)

during a single summer (2013). How robust are the δ^{18}O-S mixing relationships we have defined using the 2013 data? In this section, we conduct similar linear regressions using data sets collected by numerous projects over a period of > 15 years.

As noted in section 2, a second cruise was conducted in 2015 that re-occupied some of the transects surveyed in 2013 (i.e., SAT, L1, L5, and L6). The 2015 data suggest a very similar hydrographic setting as that encountered in 2013 (i.e., weak/absent CHL with similar cross-slope fronts observed at repeated transects). The salinity-δ^{18}O data generally agree with the scheme proposed here (see Supplementary Tables S2 & S3) as they plot along the three branches characterized using the 2013 data (Fig. 6a). For example, the regression coefficients computed using data collected from transects SAT and L1 in 2015 are very similar to those defining the SIM branch. Similarly, regression coefficients computed from data collected along transects L5 and L6 in 2015 closely resemble the upper ($S \geq 34.5$) and lower ($34 \leq S < 34.5$) MW branches. The similarity in δ^{18}O-S slopes and intercepts along these transects suggest similar processes are responsible for the transition between the SIM and MW mixing regimes and that the location of the front marking this transition likely occurred in a similar region (i.e., between transects L1 and L5, in the vicinity of SZ).

We further test the stability of these δ^{18}O-S mixing regimes by estimating linear regressions for these two salinity ranges using data collected as part of the North Pole Environmental Observatory (NPEO) (Alkire et al., 2015), Leg 2 of the ARK-XXII expedition (Bauch et al., 2011), and from the O-18 Atlas (Schmidt et al., 1999). The locations of the water samples collected during these three projects are shown in Fig. 2. The O-18 Atlas data were restricted to a latitude range of 75-90ºN and longitude range of 65-160ºE to more closely match the general area (Siberian shelves and the Nansen, Amundsen, and Makarov Basins) surveyed during the 2013 and 2015 cruises. The salinity-δ^{18}O data collected by each of these three programs all generally plot along the three mixing lines defined using the 2013 data (Fig. 6b-d). Furthermore, the regression coefficients from the upper ($S > 34.5$) and lower ($34 < S < 34.5$) salinity ranges were quite similar to those characterizing the MW branches, with the exception of the ARK-XXII expedition (Supplementary Table S4). The slope and intercept derived from the ARK-XXII data resembled the SIM mixing branch; however, a restriction of these data to the longitude range 110-160°E resulted in regression coefficients that more closely resembled the MW branch. Thus, these comparisons generally confirm the apparent dominance of the MW branch east of ~110°E (approximate position of the L3 transect) and restricted nature of the SIM branch. The similarity of the regression coefficients estimated from the NPEO (observations collected between 2000 and 2015), ARK-XXII (2007), and O-18 Atlas (1967-2008) data sets with those estimated from the 2013 and 2015 cruises further suggests that these mixing relationships have been relatively stable since at least 2000.

5 Summary & conclusions

A front was observed north of SZ at sections L3 and L4 that separated mixing branches dominated by either SIM (west of the front) or MW (east of the front). We interpret observations of salinity-δ^{18}O regressions as indicative of two stages of mixing that contribute to the formation of *basin-derived* LHW. The first stage is described by the SIM branch as AW is

Matthew Alkire 9/14/17 12:05 PM
Formatted: Font:(Default) Symbol, English (UK)

Microsoft Office User 9/19/17 3:38 PM
Deleted:

Matthew Alkire 9/14/17 12:49 PM
Formatted: Font:(Default) Times New Roman, Underline, English (UK)

Matthew Alkire 9/14/17 12:49 PM
Formatted: Font:(Default) Times New Roman, Underline, English (UK)

Matthew Alkire 9/14/17 1:07 PM
Formatted: Font:(Default) Symbol, English (UK)

Matthew Alkire 9/20/17 8:35 PM
Deleted: A cross-shore front was observed north of SZ at sections L3 and L4 that separated mixing branches dominated by either SIM (inshore) or MW (offshore). Both LHW (S~34.4) and the θ_{max} marking the AW core were relatively cooler at stations inshore of the front. Upstream at transects L1 and L2, colder halocline waters originating from the Barents Sea were generally found at stations inshore of the ~1600 m isobath (in agreement with Aksenov et al., 2011) whereas those farther offshore were either clearly dominated by warmer, FSB AW or exhibited mixing between the warmer FSB and colder BSB waters; however, no such fronts occurred in δ^{18}O-S (all stations plotted along the SIM branch). Downstream at the L5 section, three stations inshore of the ~1250 m isobath (< 77.2 °N) exhibited BSB-like θ-S characteristics but anomalously low δ^{18}O values (≤ -0.2 ‰) between salinities 34.4 and 34.7 indicating large contributions of brine. All other stations on L5 plotted along the MW branch. Thus, if BSB LHW was advected within the ASBB, it was restricted to the shallowest depths encountered during the 2013 and 2015 cruises and likely undergoes additional modification through interaction with shelf waters. Farther east at transects L5.5 and L6, stations generally plotted along the MW branch but exhibited signs of additional modification.

Matthew Alkire 9/18/17 12:44 PM
Deleted: these

Matthew Alkire 9/18/17 12:44 PM
Formatted: Font:(Default) Symbol, English (UK)

Matthew Alkire 9/15/17 1:47 PM
Deleted: *convective*

Matthew Alkire 9/15/17 1:47 PM
Formatted: Font:(Default) Times New Roman, Italic, English (UK)

freshened predominately by ice melt and is then subject to further modification through subsequent vertical mixing (with less saline, overlying waters) and ice formation. The vertical mixing reduces both salinity and $\delta^{18}O$ of the WML and ice formation then increases the salinity but only slightly decreases the $\delta^{18}O$ (see Fig. 5e). This process results in a shift from the SIM branch to the MW branch north of SZ and causes a prominent break in the salinity-$\delta^{18}O$ slope at $34.4 \leq S \leq 34.5$. The second stage is described by mixing with Siberian shelf waters containing large influences from MW and brine (negative SIM) that isolates the LHW from surface processes and builds the CHL, resulting in another change in $\delta^{18}O$-salinity slope. Farther east at transects L5.5 and L6, stations generally plotted along the MW branch but exhibited signs of additional modification that are likely a consequence of mixing with East Siberian Sea shelf waters that contain larger influences from SIM. A comparison of these results with recent studies raises questions as to whether the LHW types identified by Bauch et al. (2016) are independent, advective sources of LHW or products of mixing between *basin-derived* LHW and less saline shelf waters. Additional observations are necessary to further address these distinctions.

We also note that colder waters originating from the Barents Sea were generally found at stations inshore of the ~1600 m isobath (in agreement with Aksenov et al., 2011) along transects L1 and L2 whereas stations farther offshore were either clearly dominated by warmer, FSB AW or exhibited mixing between the warmer FSB and colder BSB waters. However, no such fronts occurred in $\delta^{18}O$-S (all stations plotted along the SIM branch). At the L5 section, three stations inshore of the ~1250 m isobath (< 77.2 °N) exhibited BSB-like θ-S characteristics but anomalously low $\delta^{18}O$ values (< -0.2 ‰) between salinities 34.4 and 34.7 indicating large contributions of brine. All other stations on L5 plotted along the MW branch. Thus, if BSB LHW was advected within the ASBB, it was restricted to the shallowest depths encountered during the 2013 and 2015 cruises and likely underwent additional modification through interaction with shelf waters. Thus, *basin-derived*, FSB LHW was the dominant LHW variety observed throughout most of our study area.

Finally, comparisons against other data sets collected across the Eurasian Basin of the Arctic Ocean (see Fig. 6) suggest that the salinity-$\delta^{18}O$ mixing regimes defined here have remained relatively stable despite changes to the sea ice cover (Polyakov et al., 2017), the temperature and volume of AW inflow (e.g., Polyakov et al., 2012a), and distribution of river runoff (Guay et al., 2001; Dmitrenko et al., 2005) for > 15 years. The apparent, robust nature of the salinity-$\delta^{18}O$ mixing regimes suggests that the processes responsible for LHW formation and modification have not been greatly altered by these important environmental changes, perhaps due to seasonal processes such as river discharge and sea-ice melting and freezing that may be delayed or diverted but not otherwise impacted by these changes. Instead, we speculate that such changes might alter the position of the front(s) marking the transition between the SIM and MW branches and/or result in data plotting in different positions along the established mixing lines (e.g., closer to or farther away from the AW endmember in salinity-$\delta^{18}O$ space). Thus, while the distribution and/or strength of stratification provided by the halocline in certain regions (e.g., Amundsen Basin) is altered by such changes, the processes responsible for halocline water formation remain consistent.

Matthew Alkire 9/18/17 12:45 PM
Deleted: space

Matthew Alkire 9/18/17 12:45 PM
Deleted: in the salinity range

Matthew Alkire 9/18/17 12:46 PM
Deleted: ,

Matthew Alkire 9/20/17 8:39 PM
Deleted: bend

Matthew Alkire 9/20/17 8:39 PM
Deleted: the

Matthew Alkire 9/20/17 8:39 PM
Deleted: relatio

Matthew Alkire 9/18/17 12:46 PM
Deleted: n and isolates the LHW from surface processes

Matthew Alkire 8/2/17 11:42 AM
Deleted: Comparisons against other data sets collected between 2000 and 2015 suggest that the salinity-$\delta^{18}O$ mixing regimes defined here remain relatively stable despite changes to the sea ice cover (Polyakov et al., 2017), the temperature and volume of AW inflow (e.g., Polyakov et al., 2012a), and distribution of river runoff (Guay et al., 2001; Dmitrenko et al., 2005). Instead, we speculate that such changes might alter the front(s) marking the transition between the SIM and MW branches.

Matthew Alkire 9/18/17 12:46 PM
Deleted: *convectively formed*

Matthew Alkire 9/18/17 12:46 PM
Formatted: Font:(Default) Times New Roman, Italic, English (UK)

Matthew Alkire 9/20/17 8:43 PM
Formatted: Font:(Default) Times New Roman, Italic, English (UK)

This implies that salinity-$\delta^{18}O$ relationships may be a more reliable method for characterizing halocline water formation and mixing during periods of significant variability.

Data availability

All data presented and/or described in this manuscript can be accessed via the National Science Foundation Arctic Data Center (https://arcticdata.io) via the following six data and metadata sets:

Igor Polyakov. 2016. NABOS - CTD Survey Data 2013. Arctic Data Center. doi:10.18739/A2M37F.

Igor Polyakov. 2016. NABOS - Water Quality and Physical Oceanography Data from the Eastern Eurasian and Makarov Basins, and Northern Laptev and East Siberian Seas in 2013. Arctic Data Center. doi:10.18739/A2G95H.

Igor Polyakov. 2016. NABOS - Chemistry Data 2013. Arctic Data Center. doi:10.18739/A2QS91.

Igor Polyakov. 2016. NABOS II - Water Quality and Physical Oceanography Data from the Eastern Eurasian and Makarov Basins, and Northern Laptev and East Siberian Seas in 2013 - 2015. Arctic Data Center. doi:10.18739/A20955.

Igor Polyakov. 2016. NABOS II - CTD Survey Data 2015. Arctic Data Center. doi:10.18739/A2436Q.

Igor Polyakov. 2016. NABOS II - Chemistry Data 2015. Arctic Data Center. doi:10.18739/A27S9P.

Matthew Alkire 8/2/17 7:51 PM
Deleted: .

Competing interests

The authors declare that they have no competing interests

Acknowledgements

Alkire acknowledges funding from the National Science Foundation (PLR-1203146 AM003) and the National Oceanic & Atmospheric Administration (NA15OAR4310156). Alkire would also like to thank Dr.'s Michael Steele and Rebecca Woodgate (Applied Physics Laboratory) for helpful comments and suggestions during the preparation of this manuscript as well as Wendy Ermold for help in figure preparation. Ivanov acknowledges funding from the Ministry of Education and Science of the Russian Federation (project RFMEFI61617X0076).

References

Aagaard, K., L. K. Coachman, and E. C. Carmack: On the pycnocline of the Arctic Ocean, Deep-Sea Research, 28, 529-545, 1981.

Alkire, M.B., Morison, J., and Andersen, R.: Variability and trends in the meteoric water, sea-ice melt, and Pacific water contributions to the central Arctic Ocean, 2000-2013, Journal of Geophysical Research, 120, 1573-1598, 2015.

Aksenov, Y., V.V. Ivanov, A.J. George Nurser, S. Bacon, I.V. Polyakov, A.C. Coward, A.C. Naveira Garabato, and A. Beszczynska Moeller: The Arctic Circumpolar Boundary Current, Journal of Geophysical Research, 116, C09017, doi:10.1029/2010JC006637, 2011.

Anderson, L.G., P.S. Andersson, G. Björk, E.P. Jones, S. Jutterström, and I. Wåhlström: Source and formation of the upper halocline of the Arctic Ocean, Journal of Geophysical Research, 118, doi:10.1029/2012JC008291, 2013.

Bauch, D. R. van der Loeff, M. Michiel, N. Andersen, S. Torres-Valdes, K. Bakker, and E.P. Abrahamsen: Origin of freshwater and polynya water in the Arctic Ocean halocline in summer 2007, Progress in Oceanography, 91(4), 482-495, doi:10.1016/j.pocean.2011.07.017, 2011.

Bauch, D., J.A. Hölemann, A. Nikulina, C. Wegner, M.A. Janout, L.A. Timokhov, and H. Kassens: Correlation of river water and local sea-ice melting on the Laptev Sea shelf (Siberian Arctic), Journal of Geophysical Research, 118, doi:10.1002/jgrc.20076, 2013.

Bauch, D., S. Torres-Valdes, I. Polyakov, A. Novikhin, I. Dmitrenko, J. McKay, and A. Mix: Halocline water modification and along-slope advection at the Laptev Sea continental margin, Ocean Science, 10, 141-154, 2014.

Bauch, D., E. Cherniavskaia, and L. Timokhov: Shelf basin exchange along the Siberian continental margin: modification of Atlantic Water and Lower Halocline Water, Deep-Sea Research I, 115, 188-198, 2016.

Bourgain, P., and J. C. Gascard: The Arctic Ocean halocline and its interannual variability from 1997 to 2008, Deep-Sea Research I, 58, 745–756, doi:10.1016/j.dsr.2011.05.001, 2011.

Cooper, L. W., McClelland, J. W., Holmes, R. M., Raymond, P. A., Gibson, J. J., Guay, C. K., and Peterson, B. J.: Flow-weighted values of runoff tracers (d18O, DOC, Ba, alkalinity) from the six largest Arctic rivers, Geophysical Research Letters, 35, doi:10.1029/2008GL035007, 2008.

Dmitrenko, I., S. Kirillov, H. Eicken, and N. Markova: Wind-driven summer surface hydrography of the eastern Siberian shelf. Geophysical Research Letters, 32, doi:10.1029/2005GL023022, 2005.

Dmitrenko, I. A., Ivanov, V. V., Kirillov, S. A., Vinogradova, E. L., Torres-Valdes, S., and D. Bauch: Properties of the Atlantic derived halocline waters over the Laptev Sea continental margin: Evidence from 2002 to 2009, Journal of Geophysical Research, 116, C10024, doi:10.1029/2011JC007269, 2011.

Eicken, H.: Deriving modes and rates of ice growth in the Wedell Sea from microstructural salinity and stable isotope data, In: Jeffries, M.O. (Ed.), Antarctic Sea Ice: Physical Processes, Interactions and Variability (Antarctic Research Series), vol. 74, AGU, Washington, D.C., pp. 89-122, 1998.

Guay, C.K., K.K Falkner, R.D. Muench, M. Mensch, M. Frank, and R. Bayer: Wind-driven transport pathways for Eurasian Arctic river discharge, Journal of Geophysical Research, 106, 11469-11480, 2001.

Jones, E. P. and Anderson, L. G.: On the origin of the chemical properties of the Arctic Ocean halocline, Journal of Geophysical Research, 91, 10759-10767, 1986.

Kikuchi, T., Hatakeyama, K., and Morison, J.: Distribution of convective Lower Halocline Water in the eastern Arctic Ocean, Journal of Geophysical Research, 109, doi:10.1029/2003JC002223, 2004.

Macdonald, R.W., Patton, D.W., and Carmack, E.C.: The freshwater budget and under-ice spreading of Mackenzie River water in the Canadian Beaufort Sea based on salinity and 18O/16O measurements in water and ice, Journal of Geophysical Research, 100, 895-919, 1995.

Melling, H., and Moore, R.M.: Modification of halocline source waters during freezing on the Beaufort Sea shelf: evidence from oxygen isotopes and dissolved nutrients, Continental Shelf Research, 15(1), 89-113, 1995.

Pfirman, S. L., Bauch, D., and Gammelsrod, T.: The northern Barents Sea: Water mass distribution and modification, In: Johannessen, O.M., R. D. Muench, and J. E. Overland (Eds.), The Polar Oceans and Their Role in Shaping the Global Environment: The Nansen Centennial Volume, Geophys. Monogr. Ser., vol. 85, pp. 77-94, AGU, Washington, D.C., 1994.

Matthew Alkire 8/2/17 11:50 AM
Deleted: 1

Matthew Alkire 8/2/17 11:50 AM
Deleted: Janout, M.A., Y. Aksenov, J.A. Hölemann, B. Rabe, U. Schauer, I.V. Polyakov, S. Bacon, A.C. Coward, M. Karcher, Y.-D. Lenn, H. Kssens, and L. Timokhov: Kara Sea freshwater transport through Vilkitsky Strait: variability, forcing, and further pathywas toward the western Arctic Ocean from a model and observations, Journal of Geophysical Research, 120, 4925-4944, doi:10.1002/2014JC010635, 2015.

Matthew Alkire 9/11/17 8:19 PM
Deleted: Kikuchi, T., Hatakeyama, K., and Morison, J.: Distribution of convective Lower Halocline Water in the eastern Arctic Ocean, Journal of Geophysical Research, 109, doi:10.1029/2003JC002223, 2004.

Polyakov, I. V., Pnyushkov, A. V., and Timokhov, L. A.: Warming of the intermediate Atlantic Water of the Arctic Ocean in the 2000s, Journal of Climate, 25(23), 8362–8370, DOI 10.1175/JCLI-D-12-00266.1, 2012a.

Polyakov, I. V., Kwok, R., and Walsh, J. E.: Recent changes of arctic multiyear sea-ice coverage and their likely causes, Bulletin of American Meteorological Society, 93(2), 145–151, DOI:10.1175/BAMS-D-11-00070.1, 2012b.

Polyakov, I.V., A.V. Pnyushkov, M.B. Alkire, I.M. Ashik, T.M. Baumann, E.C. Carmack, I. Goszczko, J. Guthrie, V.V. Ivanov, T. Kanzow, R. Krishfield, R. Kwok, A. Sundfjord, J. Morison, R. Rember, and A. Yulin: Greater role for Atlantic inflows on sea-ice loss in the Eurasian Basin of the Arctic Ocean, Science, doi:10.1126/science.aai8204, 2017.

Rudels, B., Anderson, L. G., and Jones, E. P.: Formation and evolution of the surface mixed layer and halocline of the Arctic Ocean, Journal of Geophysical Research, 101, 8807-8821, 1996.

Rudels, B., Jones, P., Schauer, U., and Eriksson, P.: Atlantic sources of the Arctic Ocean surface and halocline waters, Polar Research, 23(2), 181–208, 2004.

Schauer, U., Muench, R.D., Rudels, B., Timokhov, L.: Impact of eastern Arctic shelf waters on the Nansen Basin intermediate layers, Journal of Geophysical Research, 102(2), 3371-3382, 1997.

Schauer, U., Loeng, H., Rudels, B., Ozhigin, V.K., and Dieck, W.: Atlantic water flow through the Barents and Kara Seas, Deep-Sea Research I, 49, 2281-2298, 2002.

Schlitzer, R.: Ocean Data View. http://odv.awi.de, 2016.

Schmidt, G.A., G. R. Bigg and E. J. Rohling: Global Seawater Oxygen-18 Database - v1.21. https://data.giss.nasa.gov/o18data/, 1999.

Steele, M., Morison, J. H., and Curtin, T. B.: Halocline water formation in the Barents Sea, Journal of Geophysical Research, 100, 881-894, 1995.

Steele, M., and Boyd, T.: Retreat of the cold halocline layer in the Arctic Ocean, Journal of Geophysical Research, 103, 10 419–10 435, 1998.

Matthew Alkire 8/2/17 11:51 AM
Deleted: .

van der Loeff, M. R., P. Cai, I. Stimac, D. Bauch, C. Hanfland, T. Roeske, and S. B Moran: Shelf-basin exchange times of Arctic surface waters estimated from $^{228}Th/^{228}Ra$ disequilibrium, Journal of Geophysical Research, 117(C03024), doi:10.1029/2011JC007478, 2012.

Woodgate, R. A., Aagaard, K., Muench, R. D., Gunn, J., Bjork, G., Rudels, B., Roach, A. T., Schauer, U.: The Arctic Ocean boundary current along the Eurasian slope and the adjacent Lomonosov Ridge: water mass properties, transports and transformations from moored instruments, Deep-Sea Research I, 48, 1757-1792, 2001.

Tables

Matthew Alkire 9/15/17 11:10 AM
Formatted: Font:(Default) Times New Roman, Bold, English (UK)

Matthew Alkire 9/15/17 11:10 AM
Formatted: Font:Bold

Matthew Alkire 9/15/17 2:09 PM
Formatted: Caption

Table 1. Linear regression analyses (restricted to salinities > 34.5) of salinity-$\delta^{18}O$ measurements collected along transects occupied during the 2013. Slopes, intercepts, correlation coefficients (r) and associated standard errors (se) are reported for each transect as well as the collection of transects comprising the sea-ice melt (SIM) and meteoric (MW) water branches.

Transect	Slope	se	Intercept	se	Corrcoeff	Stations
SAT	0.2059	0.0395	-6.9306	1.3715	0.6016	109-116
L1	0.2626	0.0545	-8.8868	1.8945	0.8005	97-108
L2	0.2471	0.0292	-8.3596	1.0156	0.6656	82-91
L3 upper	0.2477	0.0373	-8.4049	1.2958	0.6919	76-81
L4 upper	0.1415	0.0412	-4.7276	1.4298	0.6632	68-69
SIM Branch	**0.2287**	**0.0347**	**-7.7306**	**1.2044**	**0.6632**	
L3 lower	0.4589	0.0424	-15.7646	1.4703	0.8864	70-75
L4 lower	0.5693	0.0577	-19.6058	2.0035	0.8776	63-66
L5	0.631	0.0379	-21.793	1.3131	0.8690	10-26 & 60-62
MW Branch	**0.6016**	**0.0321**	**-20.7517**	**1.1141**	**0.8328**	
L5.5	0.7521	0.2182	-25.9928	7.5479	0.7054	45-59
L6	0.7265	0.0924	-25.0783	3.195	0.8537	29-38

Table 2. Linear regression analyses (restricted to the salinity range: 34 < S < 34.5) of salinity-$\delta^{18}O$ measurements collected along transects occupied during the 2013. Slopes, intercepts, correlation coefficients (r) and associated standard errors (se) are reported for each transect as well as the collection of transects comprising the sea-ice melt (SIM) and meteoric (MW) water branches.

Matthew Alkire 9/15/17 2:09 PM
Formatted: Caption

Transect	Slope	se	Intercept	se	Corrcoeff	Stations
SAT	0.2361	0.0522	-7.9857	1.786	0.6863	109-116
L1	0.1113	0.225	-3.6912	7.7323	0.1266	97-108
L2	0.2048	0.063	-6.9215	2.1638	0.5105	82-91
L3 upper	0.1975	0.0605	-6.684	2.0747	0.6446	76-81
L4 upper	0.1816	0.0659	-6.1461	2.2606	0.7216	68-69
SIM Branch	**0.1871**	**0.0422**	**-6.3148**	**1.4463**	**0.6167**	
L3 lower	1.4715	0.0455	-50.6961	1.5618	0.9837	70-75
L4 lower	1.1334	0.1018	-39.0734	3.4945	0.9345	63-66
L5	1.2739	0.0462	-43.9486	1.5859	0.9356	10-26 & 60-62
MW Branch	**1.3126**	**0.0364**	**-45.2639**	**1.2482**	**0.9421**	
L5.5	0.6543	0.0822	-22.5928	2.8197	0.7411	45-59
L6	0.643	0.075	-22.2101	2.5717	0.8867	29-38

Figures

Matthew Alkire 9/15/17 12:03 PM
Formatted: Font:Bold

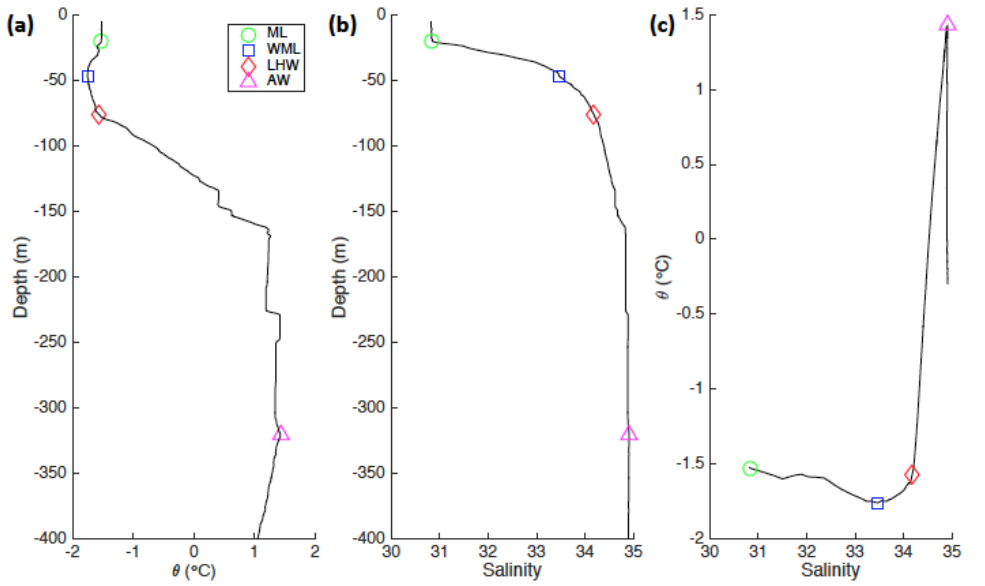

Figure 1. Vertical profiles of (a) potential temperature (θ) and (b) salinity, as well as the corresponding θ-S diagram (c) for a single station (station 26) occupied in 2013. The bottom boundaries of the surface mixed layer (SML) and winter mixed layer (WML) are shown by the green circles and blue squares, respectively. The θ-S bend (or "kink") that has been typically used to identify the position of lower halocline water (LHW) is shown by the red diamonds. The θ_{max} marking the core of the Atlantic water layer (AW) is shown by the magenta triangles. The halocline is the layer between the SML and LHW. The reverse thermocline is the layer between the LHW and AW. The base of the WML was determined as the θ_{min} below the SML. The LHW position was computed via the method outlined in Bourgain and Gascard (2011).

Matthew Alkire 9/15/17 12:03 PM
Formatted: Caption

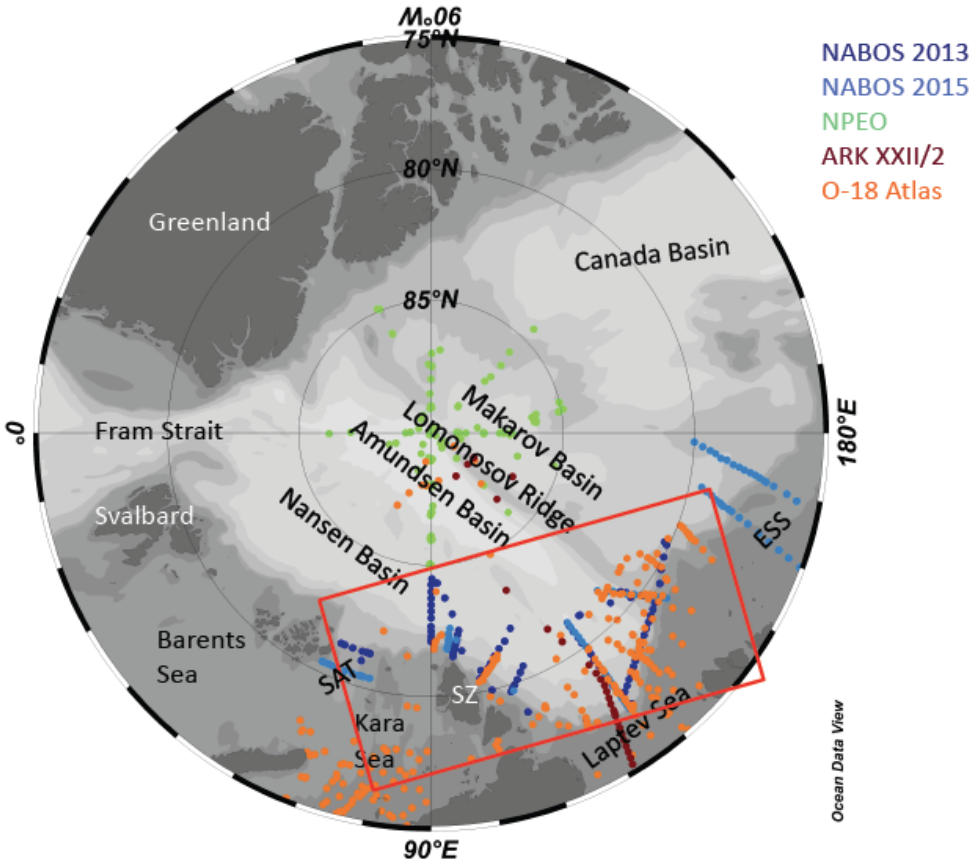

Figure 2. General map of Arctic Ocean showing study area (red box) and stations occupied during 2013 cruise (dark blue circles) and 2015 cruise (light blue circles) as well as stations occupied as part of the North Pole Environmental Observatory (green circles), ARK XXII/2 expedition (dark red circles), and O-18 Atlas (orange circles). SAT = St. Anna Trough; SZ = Severnaya Zemlya; ESS = East Siberian Sea. The map were created using Ocean Data View software (version 4.7.6) (Schlitzer, 2016).

Matthew Alkire 9/15/17 12:04 PM
Formatted: Caption

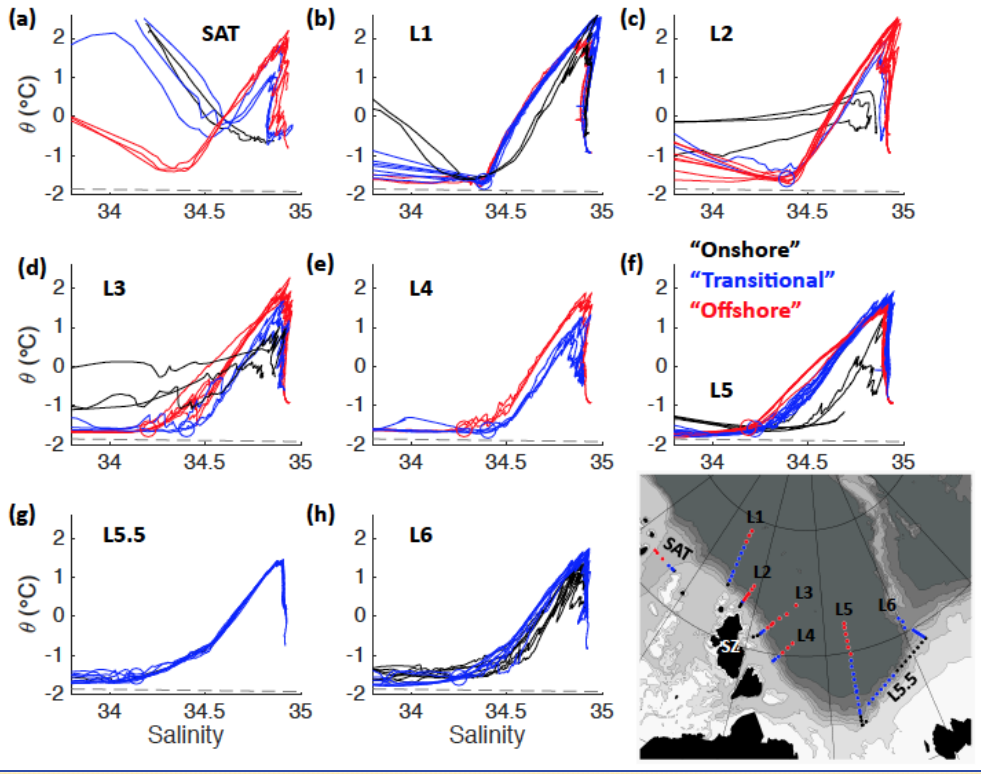

Figure 3. The panels exhibit θ-S diagrams for all data collected during the 2013 cruise. Data are divided among subpanels according to transect (SAT, L1, L2, L3, L4, L5, L5.5, and L6) with the locations of each transect shown in the inset map. The θ-S data measured at each station are colored black (closest to shore or "onshore"), blue ("transitional" between onshore and offshore), or red (farthest "offshore") according to its relative onshore vs. offshore position. Along the St. Anna Trough (SAT) section, the colors indicate the relative position of stations farthest west (red), central/east (blue), and farthest east/shallow (black) rather than onshore/offshore. The relative positions were defined differently along each transect according to fronts observed in θ-S characteristics as described in the text. Red and blue circles on these diagrams show the mean positions of LHW at the transitional and offshore stations along each transect, respectively. LHW positions along L1 and L2 did not significantly differ between transitional and offshore stations; therefore, only a single position is plotted. Note that all stations on the L6 transect were plotted in blue as there was little difference among stations indicative of a θ-S front.

Matthew Alkire 9/15/17 2:11 PM

Deleted:

Unknown

Formatted: Font:12 pt

Matthew Alkire 8/2/17 7:43 PM

Deleted: 1

Matthew Alkire 9/15/17 12:02 PM

Deleted: The top three panels illustrate vertical profiles of (a) potential temperature (θ) and (b) salinity, as well as the corresponding θ-S diagram (c) for a single station (station 26) occupied in 2013. The colored symbols show the position of the seasonal mixed layer (ML; green circle), winter mixed layer (WML; blue square), θ-S bend (or "kink") indicating the position of lower halocline water (LHW; red diamond), and the θ_{max} of the core Atlantic water (AW; magenta triangle). The cold halocline is the layer between the WML and LHW. The reverse thermocline is the layer between the LHW and AW. The WML depth was determined as the θ_{min} below the seasonal ML. The LHW position was computed via the method outlined in Bourgain and Gascard (2011).

Matthew Alkire 9/15/17 12:02 PM

Deleted: remaining

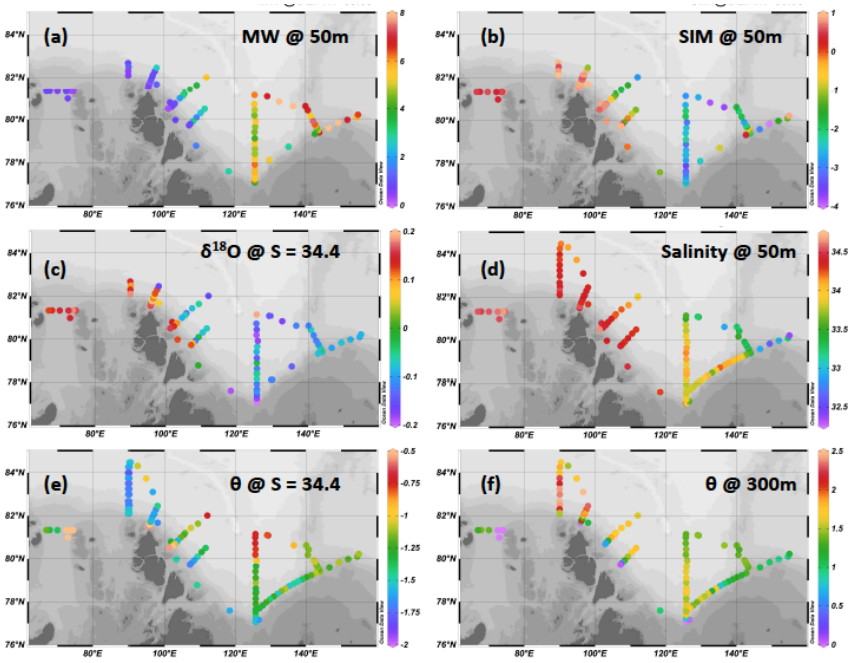

Figure 4. Maps of the (a) meteoric water (MW) fraction (%) at 50 m depth, (b) net sea-ice meltwater (SIM) fraction (%) at 50 m depth, (c) $\delta^{18}O$ (‰) on the 34.4 isohaline, (d) salinity at 50 m depth, (e) potential temperature (°C) on the 34.4 isohaline, and (f) potential temperature (°C) at 300 m (i.e., the approximate depth of the Atlantic water core). The MW and SIM fractions were calculated using a coupled water type analysis conserving salinity, $\delta^{18}O$, and mass according to methods outlined in Alkire et al. (2015); specific details regarding the methods of the analyses are provided in the Supplementary Text S2. Maps were created using Ocean Data View software (version 4.7.6) (Schlitzer, 2016).

Matthew Alkire 8/2/17 7:43 PM
Deleted: 2

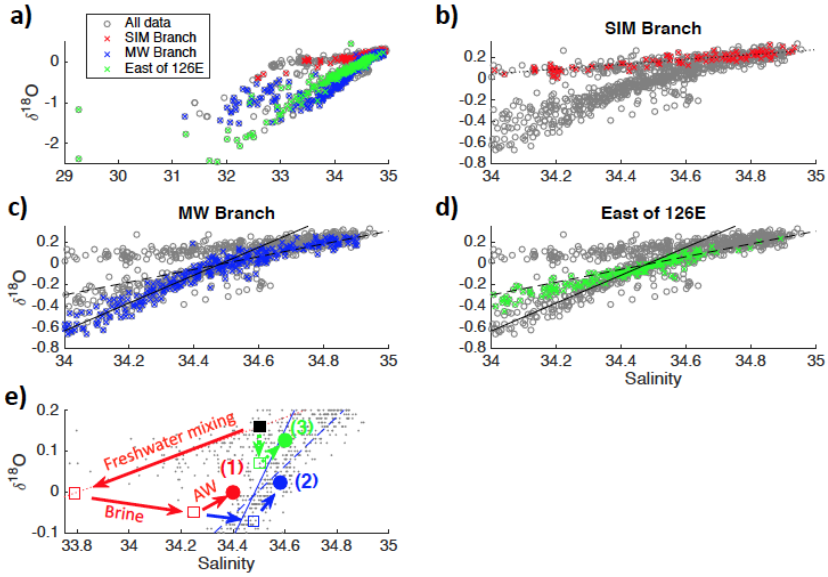

Figure 5. Plots of salinity versus the stable oxygen isotopic ratio ($\delta^{18}O$) measured during the 2013 cruise. The entire data set is plotted in each panel as gray circles. Data collected from stations comprising the sea-ice meltwater (SIM) branch, meteoric water (MW) branch, and remaining stations located east of the L5 transect (L5.5 and L6 transects) are plotted as red, blue, and green x's in panels (b), (c), and (d), respectively. Linear regressions characterizing the SIM ($\delta^{18}O = 0.2287*S - 7.7306$; $R^2 = 0.44$) and MW ($\delta^{18}O = 0.6016*S - 20.7517$; $R^2 = 0.69$) branches ($S \geq 34.5$) are plotted as dotted and dashed lines, respectively. The lower MW branch ($34 \leq S < 34.5$) is plotted as a solid line ($\delta^{18}O = 1.3126*S - 45.2639$; $R^2 = 0.89$). Both MW branches are plotted in panel (d) for comparison against data along L5.5 and L6 transects. Note that the inclusion of all data collected east of 126°E results in a linear regression that was statistically indistinguishable from the MW branch ($\delta^{18}O = 0.63S - 21.8$; $R^2 = 0.71$); however, this was not the case for the lower salinity range; thus, these stations were excluded in the definition of the MW branches. Panel (e) illustrates the transition from the SIM branch to the MW branch via mixing with overlying freshwaters, salinization through sea ice formation/brine release, and mixing with Atlantic waters (AW). The red pathway illustrates the effect of vertical mixing down to ~50 m (the mean winter mixed layer depth at SIM branch stations), brine expulsion due to the formation of 1 m of sea ice, and mixing with AW in a 21:79 ratio to form lower halocline water with a salinity of 34.4 and $\delta^{18}O$ of 0 ‰ (1). The blue pathway deviates from the red pathway due to additional ice formation (1.5 m instead of 1 m) to form lower halocline water with a salinity of 34.58 and $\delta^{18}O$ of 0.02 ‰ (2). The green pathway illustrates the effect of vertical mixing to 100 m, 1 m of sea ice formation, and AW mixing to form lower halocline water with a salinity of 34.6 and $\delta^{18}O$ of 0.13 ‰ (3). Empty squares indicate transition points after each step whereas filled circles indicate the final halocline water product formed by the three potential pathways. All three pathways yield salinity and $\delta^{18}O$ combinations near (but not directly on) the MW mixing branches, indicating some additional processes and/or mixing (such as freshwater influence from river runoff) takes place during the transition from the SIM branch to the MW branch. A larger version of this figure is available in the Supplementary Information, Figure S1.

Matthew Alkire 8/2/17 7:43 PM
Deleted: 3

Matthew Alkire 9/15/17 2:12 PM
Deleted: 6

Matthew Alkire 9/15/17 2:12 PM
Deleted: 5

Matthew Alkire 9/15/17 2:13 PM
Deleted: 5

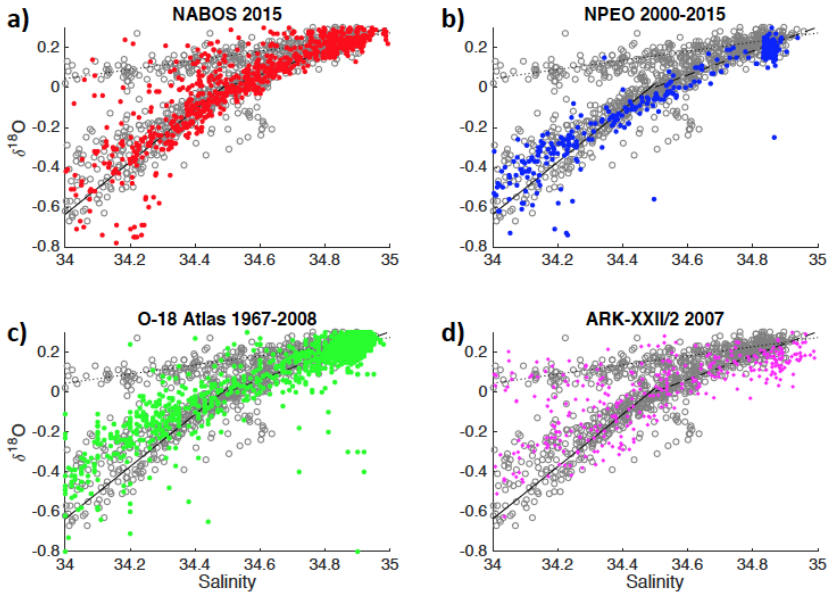

Figure 6. Comparison of data and linear regressions defining the SIM, MW, and lower MW branches defined during the 2013 cruise against additional data sets collected within the study region and in the deep basins of the eastern Arctic (Nansen, Amundsen, and/or Makarov Basins): (a) 2015 cruise; (b) North Pole Environmental Observatory (NPEO); (c) Oxygen-18 Database; and (d) ARK-XXII/2 expedition. In each panel, the 2013 data are plotted as gray circles and the linear regressions are plotted as dotted (SIM Branch), dashed (MW Branch), and solid (lower MW branch) lines. Data from each of the four cruises are plotted as (a) red, (b) blue, (c) green, and (d) magenta dots to indicate the general correspondence of these data with the mixing regimes defined by the three branches. Station locations corresponding to each data set are shown in Fig. 2. The NPEO data was previously published by Alkire et al. (2015) and can be accessed online at the NSF Arctic Data Center (https://arcticdata.io). The 2015 NABOS cruise data can be accessed online at the NSF Arctic Data Center. Data from the Oxygen-18 Database (Schmidt et al., 1999) were restricted to longitudes 65-160 ºE and latitudes 75-90 ºN to closely resemble the area sampled for this study. The data can be accessed online at https://data.giss.nasa.gov/o18data/. Data from the ARK-XXII/2 cruise aboard the *Polarstern* were published by Bauch et al. (2011) and can be accessed online via PANGEA (doi:10.1594/PANGAEA.763451).

Matthew Alkire 8/2/17 7:43 PM
Deleted: 4

Matthew Alkire 9/15/17 2:16 PM
Formatted: Font:9 pt, Bold, No underline, Font color: Auto

Unknown
Field Code Changed

Matthew Alkire 9/15/17 2:16 PM
Formatted: Font:9 pt, Bold

Unknown
Field Code Changed

Matthew Alkire 9/15/17 2:15 PM
Formatted: Font:9 pt, Bold

Matthew Alkire 9/15/17 2:15 PM
Formatted: Font:9 pt, Bold, No underline, Font color: Auto

Contents of this file

Text S1 to S2
Tables S1 to S4
Figures S1 to S4

Introduction

The following supporting information includes text describing the instruments and methods used for data collection (Text S1) and the water type analysis used to estimate fractional contributions of meteoric water, net sea-ice meltwater, and Atlantic water to each discrete water sample collected during the 2013 and 2015 cruises (Text S2). Table S1 summarizes the winter mixed layer depths and estimates of the mean salinities and potential temperatures of the subsequent winter mixed layer. Additional tables summarize linear regressions of salinity and stable oxygen isotope ratio ($\delta^{18}O$) data in specified salinity ranges from the 2015 cruise (Tables S2 and S3) and additional data sets for comparison (Table S4). Figure S1 provides a schematic of salinity and $\delta^{18}O$ changes that take place during the transition of halocline waters from the sea-ice melt branch mixing regime to the meteoric water branches as a result of mixing with overlying freshwaters, brine expulsion during ice formation, and mixing with underlying Atlantic waters. Figure S2 compares the salinity and $\delta^{18}O$ data collected during the 2013 cruise data and used to define mixing relationships in the salinity range $34 \leq S < 34.5$ against the salinity and $\delta^{18}O$ characteristics of lower halocline water types defined by *Bauch et al*., [2016]. Figures S3 and S4 provide vertical profiles of potential temperature and salinity from selected stations occupied during the 2013 cruise.

Matthew Alkire 9/15/17 11:13 AM
Deleted: S5

Matthew Alkire 9/18/17 1:53 PM
Deleted: 2

Matthew Alkire 9/15/17 2:01 PM
Deleted:

Matthew Alkire 9/15/17 2:01 PM
Deleted: Included

Matthew Alkire 9/15/17 2:00 PM
Deleted: 2013 cruise (Tables S1 and S2),

Matthew Alkire 9/15/17 2:00 PM
Deleted: 4

Matthew Alkire 9/15/17 2:00 PM
Deleted: 5

Matthew Alkire 9/15/17 2:00 PM
Deleted: ,

Matthew Alkire 9/15/17 2:00 PM
Deleted: 6

Matthew Alkire 9/15/17 2:00 PM
Deleted: Table S3 summarizes the winter mixed layer depths and estimates of the mean salinities and potential temperatures of the subsequent winter mixed layer.

Text S1. Full description of instrumentation and water sampling methods employed during the 2013 and 2015 cruises.

The sensor suite utilized during the 2013 and 2015 cruises included a Seabird SBE9*plus* conductivity-temperature-depth (CTD) equipped with dual temperature (SBE3), conductivity (SBE4), and dissolved oxygen (SBE43) sensors, SBE5T submersible pump, and a digi-quartz pressure sensor. Additional channels of the CTD system were directly connected to external sensors mounted on the carousel, including a WET Labs ECO-FLNTU chlorophyll and turbidity sensor, a WET Labs C-Star transmissometer (beam transmission and attenuation), a photosynthetically-active radiation (PAR) sensor (Biospherical model QCP2350), and a Satlantic Deep Submersible Ultraviolet Nitrate Analyzer (SUNA). A Benthos PSA-916 altimeter was also mounted to the bottom of the rosette to avoid hitting the carousel on the seafloor. Finally, twenty-four Niskin bottles (10 L capacity) were included for the collection of water samples at specified depths. All instruments were levelly mounted in the bottom section of the carousel directly below the Niskin bottles. Data was monitored and acquired during each cast using a Seabird SBE11*plus* Deck Unit.

During each cast, the rosette was moved outside to the starboard (2013) or port side (2015) deck from either a warmed container on deck using a wheeled cart (2013) or from the hydrology lab inside the ship using a hydraulic crane (2015). The rosette was then transferred to a winch and lowered over the side of the vessel to a depth of ~15 m for initialization and sensor equilibration. The rosette was then brought up to the surface (0-3 m) and then lowered through the water column at a relatively constant rate to a depth of either ~1000 m or between 5 and 20 m above the bottom (most casts were conducted to ~1000 m as some instruments cannot withstand pressures exceeding 1000 db). Once the maximum depth was reached, the rosette was stopped and a Niskin bottle was fired to obtain a water sample. The rosette was then brought back up through the water column and routinely stopped at depths of 500, 250, 200, 150, 140, 130, 120, 110, 100, 90, 80, 70, 60, 50, 40, 30, 20, 10, and 2-4 m (surface) for the collection of water samples (alternate or additional depths were tripped on a cast-by-cast basis). The rosette was stopped for a period of ~30 seconds before sample collection to allow the bottles to soak and minimize turbulent flows caused the carousel's wake as it moved upward through the water column. Once the rosette reached the surface, it was brought back on deck and transferred inside the hydrology lab using the crane.

Salinity samples were collected into 125-mL glass bottles equipped with polyethylene inserts to prevent evaporation. In 2013, salinity samples were analyzed via salinometer onboard after a 12-hour temperature equilibration. However, unstable laboratory temperatures prevented the collection of quality data from the salinometer; thus, the bottle salinity data was not utilized from the 2013 cruise. In 2015, bottle samples (n = 93) for salinity determinations were collected and shipped back to the University of Washington for analysis using a Guideline 8400B salinometer (calibrated with IAPSO standard seawater) at the Marine Chemistry Laboratory (UW Oceanography). The majority (76 %) of bottle salinities differed from CTD salinities by $\leq$ 0.04, though larger discrepancies did occur (49 % of available comparisons indicated differences of $\leq$ 0.01 and 86 % indicated differences $\leq$ 0.1).

Text S2: Full description of water type analysis methods.

Fractional contributions of meteoric water (MW) and net sea-ice meltwater (SIM), and a saline water endmember (Atlantic seawater, AW, for the purposes of this study) can be quantified using salinity and $\delta^{18}O$ observations in a set of coupled equations that also conserves mass (or volume):

$$S_{SIM} \times f_{SIM} + S_{MW} \times f_{MW} + S_{AW} \times f_{AW} = S_{obs} \quad (1)$$

$$\delta^{18}O_{SIM} \times f_{SIM} + \delta^{18}O_{MW} \times f_{MW} + \delta^{18}O_{AW} \times f_{AW} = \delta^{18}O_{obs} \quad (2)$$

$$f_{SIM} + f_{MW} + f_{AW} = 1 \quad (3)$$

where f equals the fractional contributions of the three water types (i.e., SIM, MW, and AW) and *S* and $\delta^{18}O$ represent the characteristic salinities and stable oxygen isotopic ratios associated with these water types. Note that net sea-ice formation (formation exceeding melting) will generate a negative SIM fraction ($f_{SIM} < 0$), representing an extraction of liquid water into the solid phase (ice) and the release of brine into the water column. This water type analysis assumes that salinity and $\delta^{18}O$ values that characterize MW, SIM, and AW (commonly referred to as endmember values) are well known and relatively stable over time. However, there is seasonal and interannual variability associated with these endmember values that should be taken into account when conducting a water type analysis. Thus, estimates of uncertainty in the water type fractions resulting from the analysis can be computed by varying the endmember values within reasonable ranges of natural variability. In this study, meteoric water $\delta^{18}O$ endmember values were varied between -22 and -18 ‰. The salinity of meteoric water is zero by definition. Sea-ice meltwater salinity and $\delta^{18}O$ endmember values were varied between 2 and 8 and -2 and +3 ‰, respectively. Atlantic seawater salinity and $\delta^{18}O$ endmember values were varied between 34.85 and 35 and 0.25 and 0.35 ‰, respectively.

Similar to the methods described in *Alkire et al.* [2015], the water type analysis was iterated 1,000 times for each salinity and $\delta^{18}O$ pair. The set of endmember values characterizing MW, SIM, and AW were randomly selected from the specified ranges for each iteration. Though the endmember selection was randomized, it was organized in such a way that allowed all values within each range to be selected an equal number of times. Averages of the MW, SIM, and AW fractions (1,000 values for each salinity, $\delta^{18}O$ pair) were taken as the best estimate of the water type fractions and associated standard deviations taken as estimates of uncertainties due to natural variations in the endmember assignments. The median standard deviations for MW, SIM, and AW fractions were 0.24, 0.36, and 0.20 % for the 2013 cruise and 0.29, 0.41, and 0.21 % for the 2015 cruise, respectively. Note that these uncertainties are *absolute* uncertainties (e.g., meteoric water fraction reported as 8 ± 0.24 %).

Table S1. Winter mixed layer (WML) depth, salinity, and potential temperature (θ) estimated from CTD data by identifying the minimum potential temperature below the surface mixed layer. We note that the identification of the WML depth by this method is associated with some uncertainty and may be particularly ambiguous at stations with a mixed layer close to the freezing point. The WML depths estimated using this method were visually checked against vertical profiles of potential temperature and θ-S diagrams. Stations that appeared to have no clearly identifiable θ_{min} or multiple minima are marked with "*CND*" (could not determine). "Salt mixed" and "θ mixed" refer to the mean salinities and potential temperatures estimated from individual profiles assuming the water column will be homogenized down to the previous year's WML.

Station	Transect	WML Depth (m)	WML Salinity	WML θ	Salt mixed	θ mi
1	-	52	34.556	-0.699	34.112	1.0
2	-	56	34.368	-1.674	33.867	-1.3
3	-	45	34.365	-1.384	33.876	-1.2
4	-	52	34.414	-1.533	33.849	-1.5
5	-	49	34.443	-1.485	33.563	-1.2
6	-	48	34.236	-1.663	32.940	-0.4
7	L5	*CND*	-	-	-	-
8	L5	*CND*	-	-	-	-
9	L5	85	34.282	-1.659	33.084	-0.4
10	L5	87	34.317	-1.611	33.350	-0.6
11	L5	58	34.024	-1.750	32.457	-0.5
12	L5	50	33.893	-1.792	32.896	-1.0
13	L5	64	33.896	-1.799	32.744	-1.2
14	L5	56	33.918	-1.797	32.947	-1.4
15	L5	52	34.023	-1.775	33.315	-1.6
16	L5	67	34.210	-1.727	33.573	-1.6
17	L5	53	33.968	-1.762	33.141	-1.6
18	L5	52	34.149	-1.721	33.285	-1.5
19	L5	40	33.995	-1.733	33.098	-1.622
20	L5	42	34.011	-1.747	32.939	-1.611
21	L5	59	33.994	-1.745	33.076	-1.622
22	L5	45	33.720	-1.730	32.331	-1.577
23	L5	55	33.934	-1.754	32.526	-1.627
24	L5	39	33.383	-1.770	32.022	-1.610
25	L5	68	33.838	-1.819	32.630	-1.671
26	L5	47	33.464	-1.759	31.888	-1.611
27	-	*CND*	-	-	-	-
28	-	*CND*	-	-	-	-
29	L6	70	34.022	-1.675	31.551	-1.127
30	L6	70	34.056	-1.633	31.863	-1.348
31	L6	61	33.801	-1.655	31.125	-1.320
32	L6	73	34.006	-1.664	31.556	-1.482

Matthew Alkire 9/15/17 11:12 AM
Deleted: **Table S1.** Linear regression analyses (restricted to salinities ≥ 34.5) of salinity-$\delta^{18}O$ measurements collected along transects occupied during the 2013. Slopes, intercepts, correlation coefficients (r) and associated standard errors (se) are reported for each transect as well as the collection of transects comprising the sea-ice melt (SIM) and meteoric (MW) water branches.
Transect ... [1]

Matthew Alkire 9/15/17 11:11 AM
Deleted: S3

Matthew Alkire 9/5/17 8:15 PM
Formatted: Font:Symbol

Matthew Alkire 9/5/17 8:16 PM
Formatted: Font:Symbol

Matthew Alkire 9/5/17 8:16 PM
Formatted: Subscript

Matthew Alkire 9/5/17 8:17 PM
Formatted: Font:Not Italic

Matthew Alkire 9/5/17 8:44 PM
Deleted: Station ... [2]

Matthew Alkire 9/5/17 2:59 PM
Formatted: Font:Italic

Matthew Alkire 9/5/17 2:59 PM
Formatted: Font:Italic

Matthew Alkire 9/5/17 3:01 PM
Formatted: Font:Italic

Matthew Alkire 9/5/17 8:46 PM
Formatted Table

Matthew Alkire 9/5/17 8:46 PM
Formatted: Font:Symbol

Matthew Alkire 9/5/17 8:46 PM
Formatted Table

33	L6	51	33.513	-1.717	31.162	-1.434
34	L6	46	32.992	-1.675	30.677	-1.489
35	L6	40	32.340	-1.620	30.412	-1.468
36	L6	44	33.242	-1.739	30.896	-1.532
37	L6	46	32.973	-1.731	31.124	-1.603
38	L6	75	34.020	-1.706	32.116	-1.597
39	-	59	33.150	-1.753	32.020	-1.659
40	-	44	32.557	-1.673	30.467	-1.254
41	-	46	32.484	-1.742	31.099	-1.620
42	-	39	32.494	-1.712	31.246	-1.651
43	-	37	32.202	-1.679	31.044	-1.652
44	-	52	32.384	-1.693	31.357	-1.668
45	L5.5	43	33.180	-1.600	30.802	-0.745
46	L5.5	51	33.897	-1.659	31.681	-0.435
47	L5.5	*CND*	-	-	-	-
48	L5.5	48	33.980	-1.683	32.122	-0.542
49	L5.5	63	34.234	-1.571	32.615	-0.603
50	L5.5	58	34.204	-1.591	32.590	-0.622
51	L5.5	*CND*	-	-	-	-
52	L5.5	*CND*	-	-	-	-
53	L5.5	*CND*	-	-	-	-
54	L5.5	*CND*	-	-	-	-
55	L5.5	*CND*	-	-	-	-
56	L5.5	50	33.867	-1.776	32.323	-1.124
57	L5.5	59	33.921	-1.774	32.931	-1.100
58	L5.5	63	33.961	-1.766	32.750	-0.674
59	-	65	34.051	-1.728	33.112	-0.711
60	L5	62	33.986	-1.762	32.831	-0.674
61	L5	44	33.991	-1.728	33.177	-1.271
62	L5	44	34.000	-1.737	33.045	-1.000
63	L4	*CND*	-	-	-	-
64	L4	*CND*	-	-	-	-
65	L4	26	33.959	-1.670	32.814	-1.067
66	L4	*CND*	-	-	-	-
67	L4	42	34.297	-1.688	33.673	-1.421
68	L4	51	34.334	-1.689	33.783	-1.381
69	L4	46	34.353	-1.716	33.739	-1.404
70	L3	20	32.257	-1.718	32.246	-1.714
71	L3	15	31.864	-1.718	31.864	-1.719
72	L3	*CND*	-	-	-	-
73	L3	*CND*	-	-	-	-
74	L3	31	33.955	-1.686	33.097	-1.588
75	L3	22	34.040	-1.683	33.327	-1.517

76	L3	33	34.195	-1.663	33.208	-1.602
77	L3	48	34.322	-1.681	33.715	-1.560
78	L3	52	34.354	-1.610	33.692	-1.441
79	L3	*CND*	-	-	-	-
80	L3	*CND*	-	-	-	-
81	L3	*CND*	-	-	-	-
82	L2	*CND*	-	-	-	-
83	L2	*CND*	-	-	-	-
84	L2	*CND*	-	-	-	-
85	L2	54	34.309	-1.385	33.709	-0.538
86	L2	53	34.336	-1.566	33.798	-0.783
87	L2	42	34.370	-1.545	33.711	-0.567
88	L2	55	34.360	-1.584	33.799	-0.664
89	L2	51	34.392	-1.623	33.825	-0.995
90	L2	52	34.390	-1.694	33.893	-1.255
91	L2	58	34.405	-1.723	33.800	-1.410
92	L2	*CND*	-	-	-	-
93	L2	51	34.393	-1.648	33.823	-1.166
94	-	87	34.420	-1.770	34.014	-1.624
95	-	44	33.993	-1.727	32.937	-1.689
96	-	*CND*	-	-	-	-
97	L1	*CND*	-	-	-	-
98	L1	*CND*	-	-	-	-
99	L1	85	34.366	-1.795	33.925	-1.647
100	L1	*CND*	-	-	-	-
101	L1	71	34.370	-1.764	34.050	-1.601
102	L1	58	34.367	-1.719	34.004	-1.460
103	L1	58	34.372	-1.710	33.861	-1.332
104	L1	66	34.390	-1.705	33.995	-1.409
105	L1	59	34.379	-1.728	33.942	-1.337
106	L1	30	34.363	-1.547	33.654	-0.659
107	L1	45	34.289	-1.610	33.781	-0.443
108	L1	45	34.292	-1.589	33.737	-0.198
109	SAT	*CND*	-	-	-	-
110	SAT	*CND*	-	-	-	-
111	SAT	48	34.626	-0.168	34.309	1.795
112	SAT	43	34.583	-0.213	34.245	1.788
113	SAT	42	34.526	-0.535	34.010	1.085
114	SAT	38	34.337	-1.411	33.769	-0.176
115	SAT	35	34.274	-1.355	33.708	0.080
116	SAT	39	34.322	-1.321	33.626	0.141

Averages

ALL stations	51	33.932	-1.617	32.890	-1.085
SIM Branch stations	50	34.370	-1.475	33.825	-0.719

Table S2. Linear regression analyses (restricted to salinities ≥ 34.5) of salinity-$\delta^{18}O$ measurements collected along transects occupied during the 2015. Slopes, intercepts, correlation coefficients (r) and associated standard errors (se) are reported for each transect.

Matthew Alkire 9/15/17 11:11 AM
Deleted: 4

Transect	Slope	se	Intercept	se	Corrcoeff	Stations
SAT	0.2243	0.0723	-7.5502	2.5162	0.299	81-93
L2	0.4317	0.0418	-14.8127	1.4567	0.7723	2-9 & 78-79
L5	0.6056	0.0345	-20.8911	1.1974	0.8454	10-24 & 72-76
L6	0.572	0.0436	-19.7179	1.5128	0.8763	27-38
165E	0.7238	0.147	-24.9681	5.1044	0.7017	39-54
175E	0.5906	0.104	-20.3403	3.6086	0.6777	56-71

Table S3. Linear regression analyses (restricted to the salinity range: 34 ≤ S < 34.5) of salinity-$\delta^{18}O$ measurements collected along transects occupied during the 2015. Slopes, intercepts, correlation coefficients (r) and associated standard errors (se) are reported for each transect.

Matthew Alkire 9/15/17 11:12 AM
Deleted:

Matthew Alkire 9/15/17 11:11 AM
Deleted: 5

Transect	Slope	se	Intercept	se	Corrcoeff	Stations
SAT	0.3252	0.1944	-11.0302	6.6668	0.5092	81-93
L2	0.3292	0.0839	-11.2715	2.8837	0.5887	2-9 & 78-79
L5	1.556	0.107	-53.6881	3.6745	0.8267	10-24 & 72-76
L6	1.3081	0.0716	-45.0777	2.4549	0.9048	27-38
165E	0.8079	0.0824	-27.9041	2.8254	0.8499	39-54
175E	1.1662	0.0746	-40.239	2.5568	0.9472	56-71

Table S4. Linear regression analyses of salinity-$\delta^{18}O$ measurements available from different data sets, including the North Pole Environmental Observatory (NPEO) [*Alkire et al.,* 2015], Global Seawater Oxygen-18 Database [*Schmidt et al*., 1999], and *Polarstern* cruise ARK-XXI/2 [*Bauch et al*., 2011]. Slopes, intercepts, and correlation coefficients are reported for each data set. NPEO data were collected annually between 2000 and 2015 (no data from 2009) at latitudes ≥ 85°N, primarily along longitudinal transects 90°E and 180° [*Alkire et al*., 2015]. Measurements from the O-18 Database were restricted to latitudes ≥ 75°N, and longitudes ranging between 65 and 160°E to best resemble the area studied in 2013. Further restrictions were applied, limiting the O-18 data to years after 2000 (2000, 2001, 2007, 2008) and then to 2007-2008, to determine the impact (if any) on $\delta^{18}O$-S relationships. ARK-XXII/2 data were similarly restricted to latitudes ≥ 75°N and longitudes 65-160°E. A second longitudinal restriction (110-160°E) was employed on the ARK-XXII/2 data to investigate the spatial dependence on the regression coefficients.

Data Source	Years	Salinity Range	Slope	Intercept	Corrcoef	N
NPEO	2000-2015	S ≥ 34.5	0.6690	-23.1220	0.7877	141
		34 ≤ S < 34.5	1.1423	-39.4408	0.6305	162
O-18 Database	1967-2008	S > 34.5	0.4618	-15.8776	0.5191	1350
		34 < S < 34.5	0.8635	-29.7775	0.6524	304
	2000-2008	S > 34.5	0.5401	-18.5999	0.6571	606
		34 < S < 34.5	0.9234	-31.8298	0.6757	153
	2007-2008	S > 34.5	0.6261	-21.5984	0.7091	598
		34 < S < 34.5	0.9669	-33.3287	0.7621	125
ARK-XXII/2	2007	S ≥ 34.5	0.3749	-12.9036	0.5923	104
		34 ≤ S < 34.5	0.2478	-8.6570	0.2219	113
	110-160°E	S ≥ 34.5	0.3796	-13.1062	0.4748	24
	110-160°E	34 ≤ S < 34.5	0.5205	-18.0897	0.5868	59

Matthew Alkire 9/15/17 11:11 AM
Deleted: S6

Matthew Alkire 9/14/17 2:00 PM
Deleted: those collected after 2000 (2000, 2001, 2007, 2008),

Matthew Alkire 9/14/17 2:02 PM
Formatted: Font:Symbol

Matthew Alkire 9/14/17 2:02 PM
Formatted: Superscript

Matthew Alkire 9/15/17 2:20 PM
Deleted: O-18 Database ... [3]

Matthew Alkire 9/15/17 2:22 PM
Formatted: Font:Not Italic

Matthew Alkire 9/15/17 2:22 PM
Formatted: Font:Not Italic

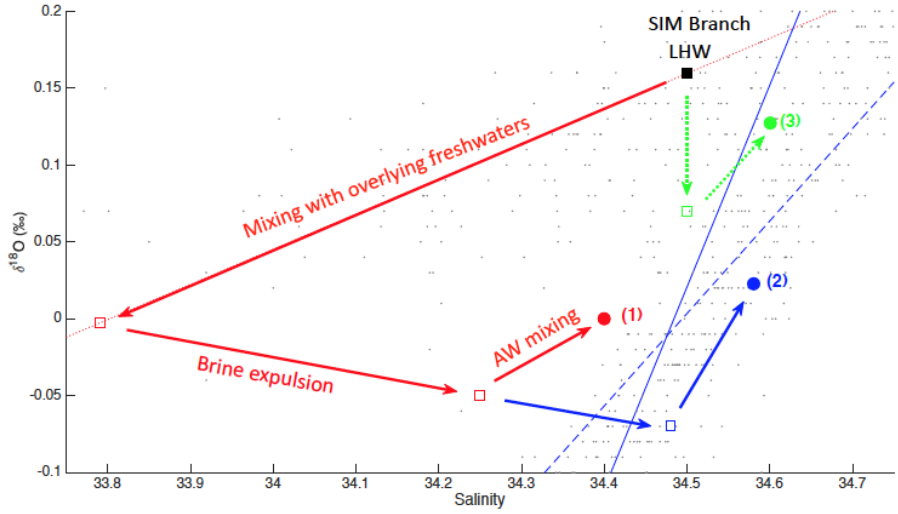

Figure S1. Schematic of the transition of lower halocline waters from the SIM branch to the MW branch via mixing with overlying freshwaters, salinization through sea ice formation/brine release, and mixing with Atlantic waters (AW). The red pathway illustrates the effect of vertical mixing down to 50 m (the mean winter mixed layer depth at SIM branch stations), brine expulsion due to the formation of 1 m of sea ice, and mixing with AW in a 21:79 ratio to form lower halocline water with a salinity of 34.4 and $\delta^{18}O$ of 0 ‰ (1). The blue pathway deviates from the red pathway due to additional ice formation (1.5 m instead of 1 m) to form lower halocline water with a salinity of 34.58 and $\delta^{18}O$ of 0.02 ‰ (2). The green pathway illustrates the effect of vertical mixing to 100 m, 1 m of sea ice formation, and AW mixing to form lower halocline water with a salinity of 34.6 and $\delta^{18}O$ of 0.13 ‰ (3). The regression lines representing the SIM branch (red, dotted line), upper MW branch (blue, dashed line), and lower MW branch (blue, solid line) are also shown for reference. The gray dots indicate data collected during the 2013 cruise. Empty squares indicate transition points after each step (freshwater mixing, brine expulsion, and AW mixing) whereas filled circles indicate the final halocline water product formed by the three potential pathways. All three pathways yield salinity and $\delta^{18}O$ combinations near (but not directly on) the MW mixing branches, indicating some additional processes and/or mixing (such as freshwater influence from river runoff) takes place during the transition from the SIM branch to the MW branch.

Matthew Alkire 9/15/17 2:05 PM
Deleted: ~

Matthew Alkire 9/15/17 2:05 PM
Deleted: 6

Matthew Alkire 9/15/17 2:05 PM
Deleted: 5

Matthew Alkire 9/15/17 2:05 PM
Deleted: 5

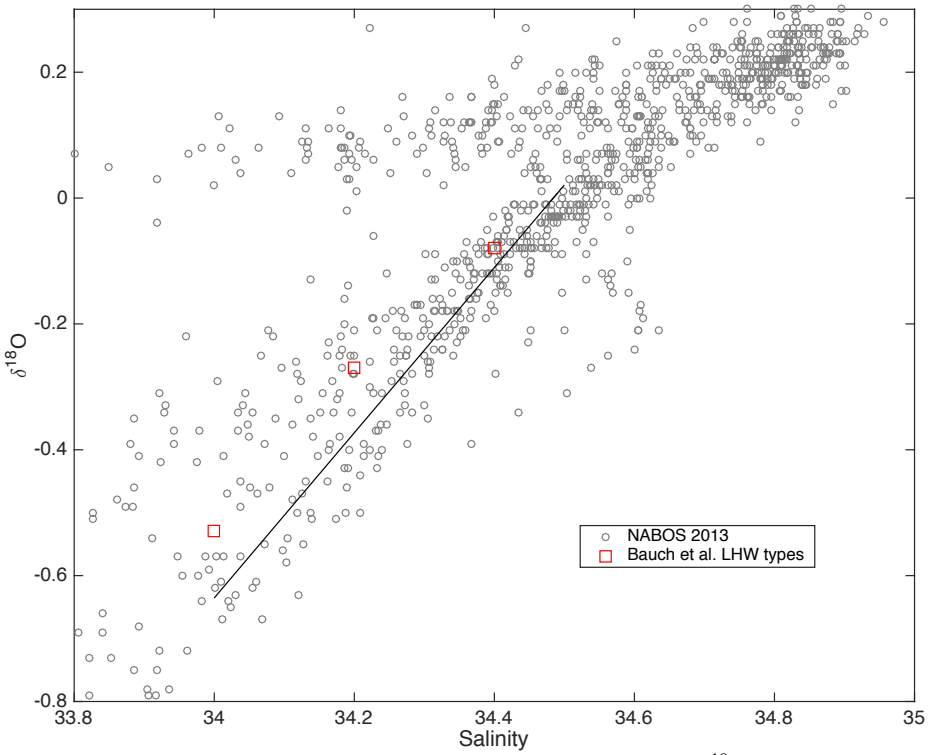

Figure S2. Plots of salinity versus the stable oxygen isotopic ratio ($\delta^{18}O$) measured during the 2013 cruise (gray circles) and characteristic values for the c2 (S = 34, $\delta^{18}O$ = -0.53‰), c3 (S = 34.2, $\delta^{18}O$ = -0.27 ‰), and c4 (S = 34.4, $\delta^{18}O$ = -0.08 ‰) lower halocline water (LHW) water types (red squares) defined in *Bauch et al.* [2016]. The c1 LHW type (S = 33.0, $\delta^{18}O$ = -1.46 ‰) is not shown. The linear regression defining the lower MW branch ($\delta^{18}O$ = 1.3126*S – 45.2639) is included as a black, solid line. Note that a separate linear regression of the values characterizing the four LHW types was $\delta^{18}O$ = 0.9828*S – 33.901.

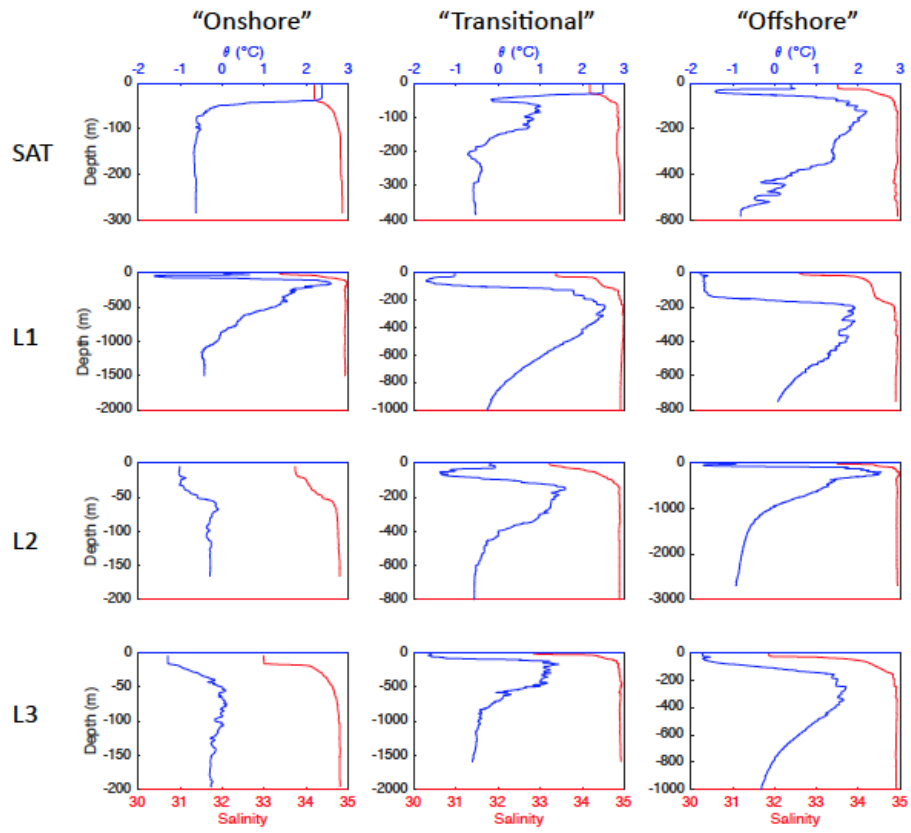

Figure S3. Vertical profiles of potential temperature (θ) and salinity plotted as blue and red lines, respectively, for selected stations on the SAT, L1, L2, and L3 transects. Stations were selected that generally represented the hydrographic conditions observed nearest the continental shelves ("onshore"), on the slope ("transitional"), and in the deep basins (offshore) along each transect. Note that, while the temperature and salinity axes are identical among panels, the range of the y-axes (depth) varies with each panel.

Matthew Alkire 9/18/17 1:46 PM
Formatted: Font:Symbol

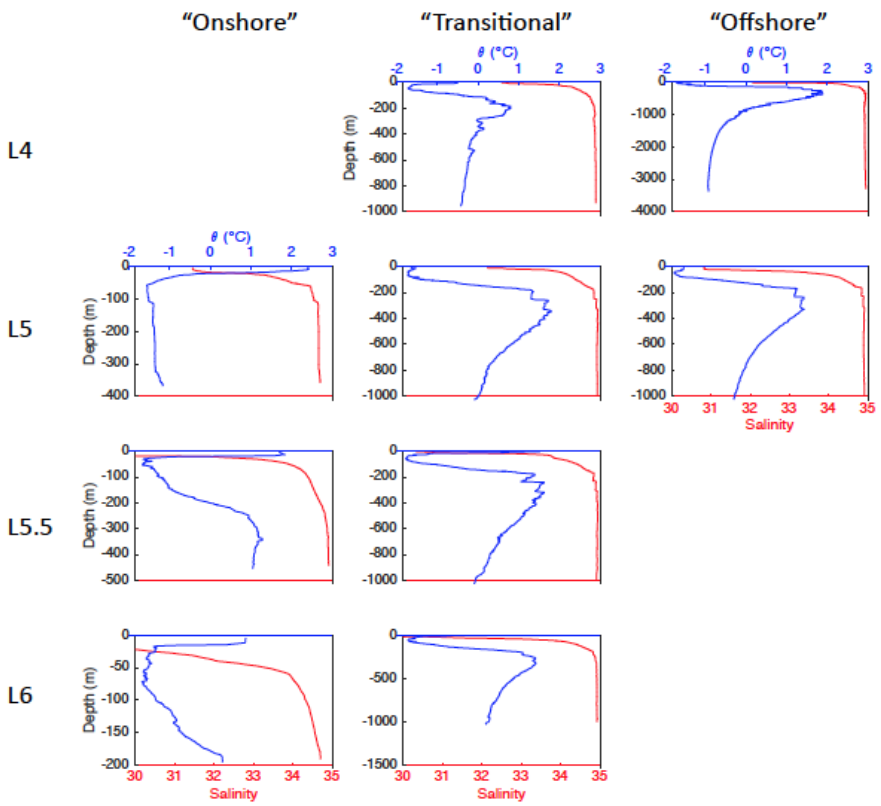

Figure S4. Vertical profiles of potential temperature (θ) and salinity plotted as blue and red lines, respectively, for selected stations on the L4, L5, L5.5, and L6 transects. Stations were selected that generally represented the hydrographic conditions observed nearest the continental shelves ("onshore"), on the slope ("transitional"), and in the deep basins (offshore) along each transect. Note that, while the temperature and salinity axes are identical among panels, the range of the y-axes (depth) varies with each panel.

Unknown
Deleted: .